PNAS
www.pnas.org

Supplementary Information for

Supplementary Information for
Dynamic coexistence driven by physiological transitions in microbial communities

Avaneesh V. Narla, Terence Hwa, and Arvind Murugan

Arvind Murugan
E-mail: amurugan@uchicago.edu
Terence Hwa
E-mail: thwa@ucsd.edu

This PDF file includes:

Figs. S1 to S10
References for SI reference citations

Contents

S1. Supplementary Figures

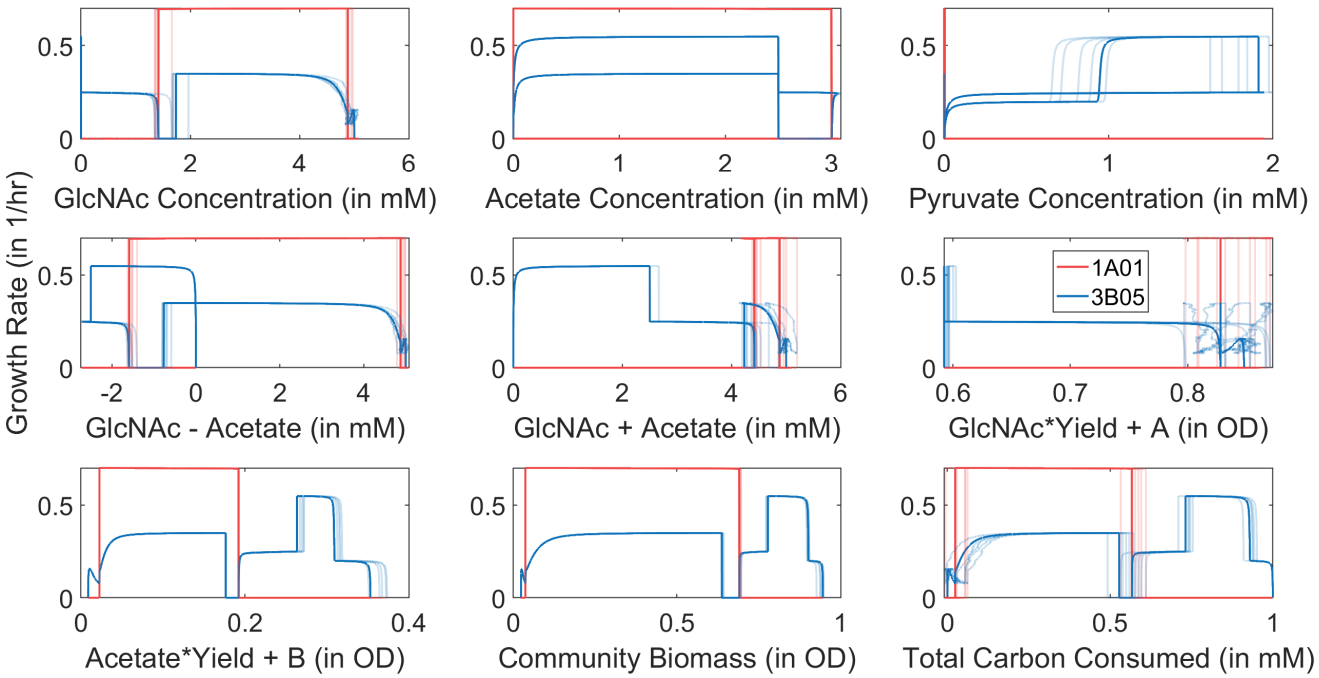

Fig. S1. Growth rate (light blue,red) along perturbed trajectories (in response to random perturbations of metabolites of size 1% every 10 mins) plotted against a range of potential eco-coordinates combining different variables of the system, compare to Fig. 1F. Growth rate along unperturbed trajectories is shown in solid blue and solid red.

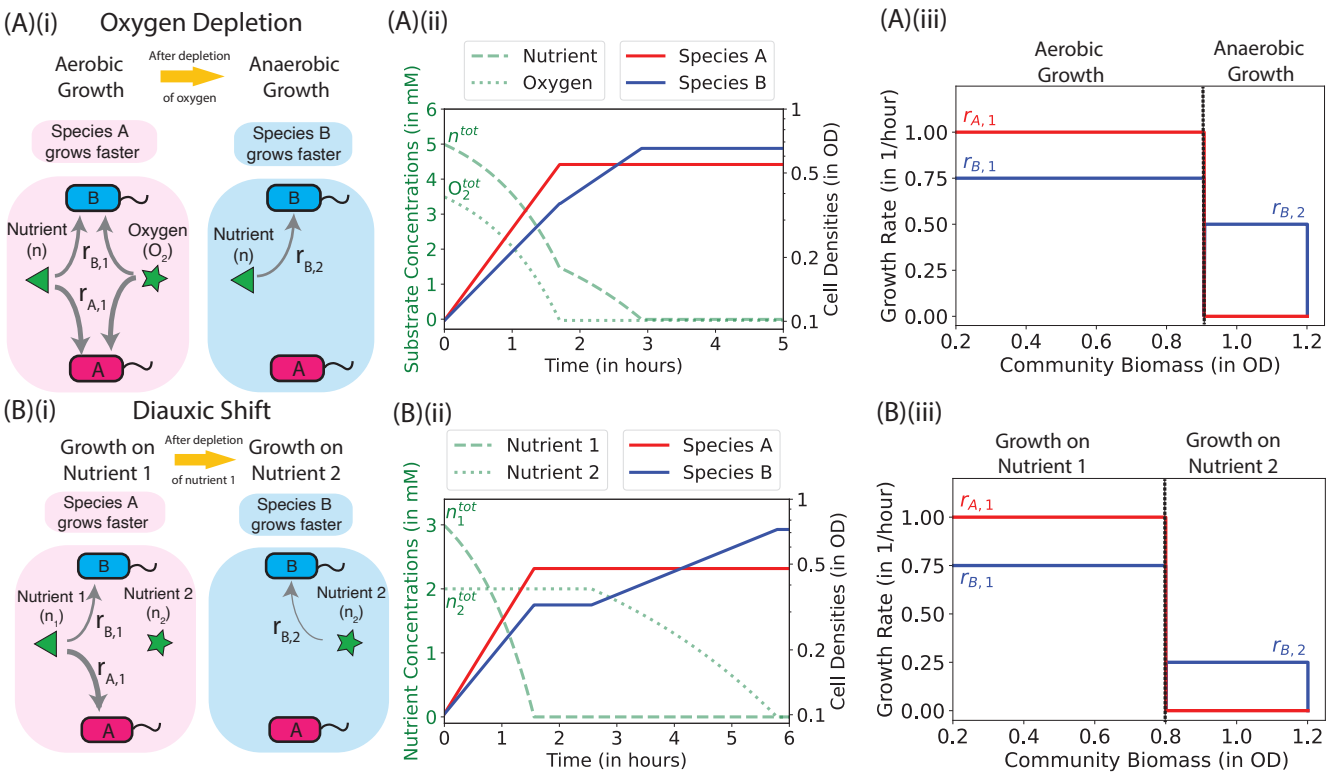

Fig. S2. Growth transitions arising in oxygen depletion and diauxic shift. Illustrations are made for two species, A (red) and B (blue), whose growth rates, r_A and r_B, respectively, vary due to changes in the concentrations of nutrients or toxins in the common media due to a variety of interactions. Growth curves are shown as red and blue solid lines in the middle column, with nutrient/toxin concentrations shown as green dashed or dotted lines. Growth rates are plotted against the accumulated total biomass density in the right column. **A.** Species A grows faster than B aerobically. However, after the depletion of oxygen, only B continues to grow anaerobically, although at a slower rate. **B.** Species A grows faster than B on nutrient 1. Species A stops growing after the depletion of nutrient 1 but B continues to grow on nutrient 2 after a classic diauxic shift, reflected by a lag in the growth curve (middle column of panel B). Note that when plotting the growth rate against the total biomass accumulated in the community, the lag does not show up as there is no biomass accumulation during this period. More such examples are provided in Fig. S3

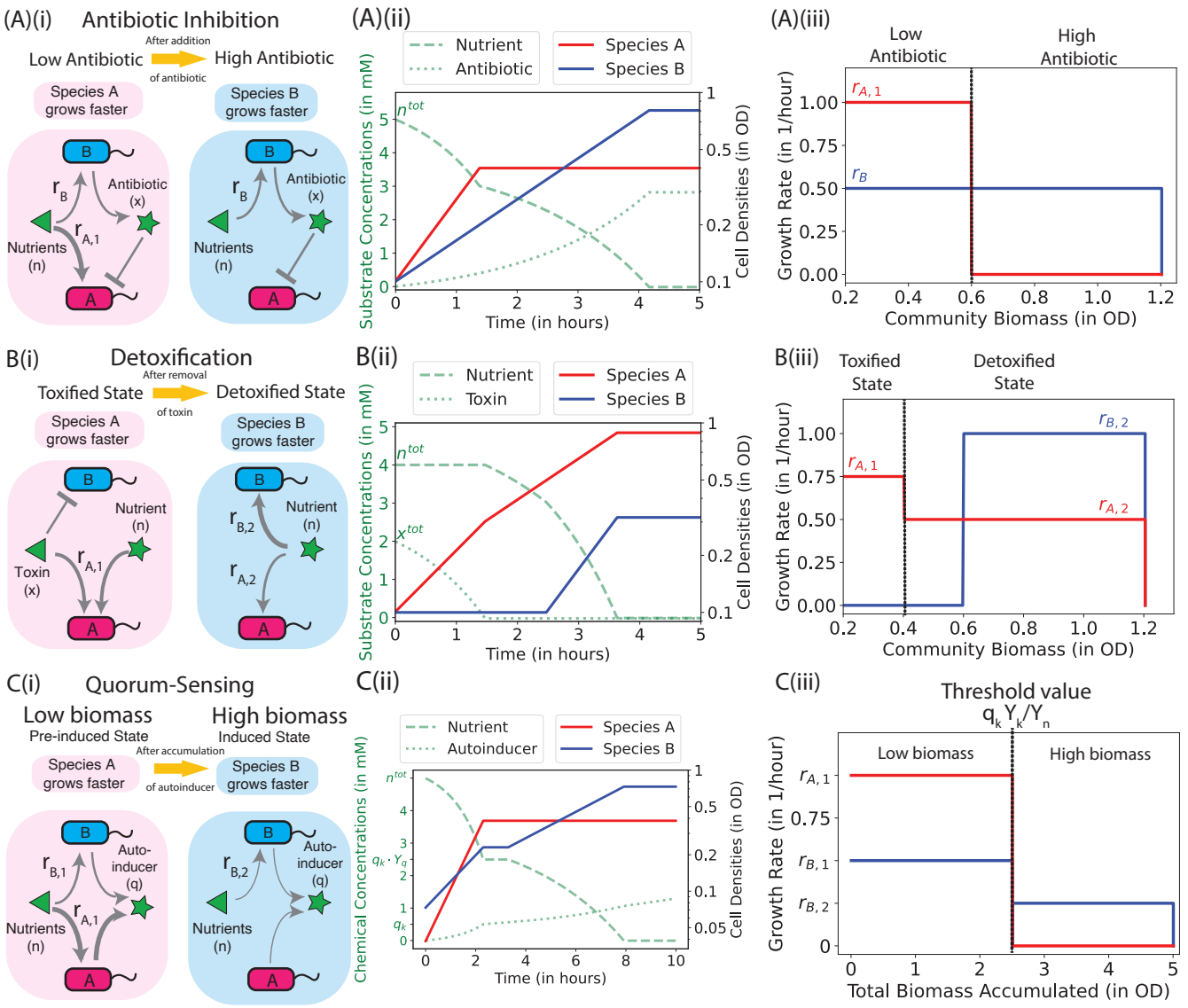

Fig. S3. Growth transitions arising in antibiotic inhibitions, detoxification, and quorum-sensing. Illustrations are made for two species, A (red) and B (blue), whose growth rates, r_A and r_B, respectively, vary due to changes in the concentrations of nutrients or toxins in the common media due to a variety of interactions. Growth curves are shown as red and blue lines in the middle column, with nutrient/toxin concentrations shown as the green dashed or dotted lines. Growth rates are plotted against the accumulated total biomass in the right column. **A.** Species A grows faster than Species B, but Species B excretes an antibiotic which inhibits the growth of Species A when accumulated to a sufficient level. B itself is not sensitive to the antibiotic. **B.** A toxin in the medium inhibits the growth of Species B, but is consumed by Species A. After toxin removal, A continues to grow (at a moderately reduced rate) while B can grow at a fast rate. **C.** Both species secrete autoinducers. After the autoinducer concentration reaches a threshold value, B grows faster than A.

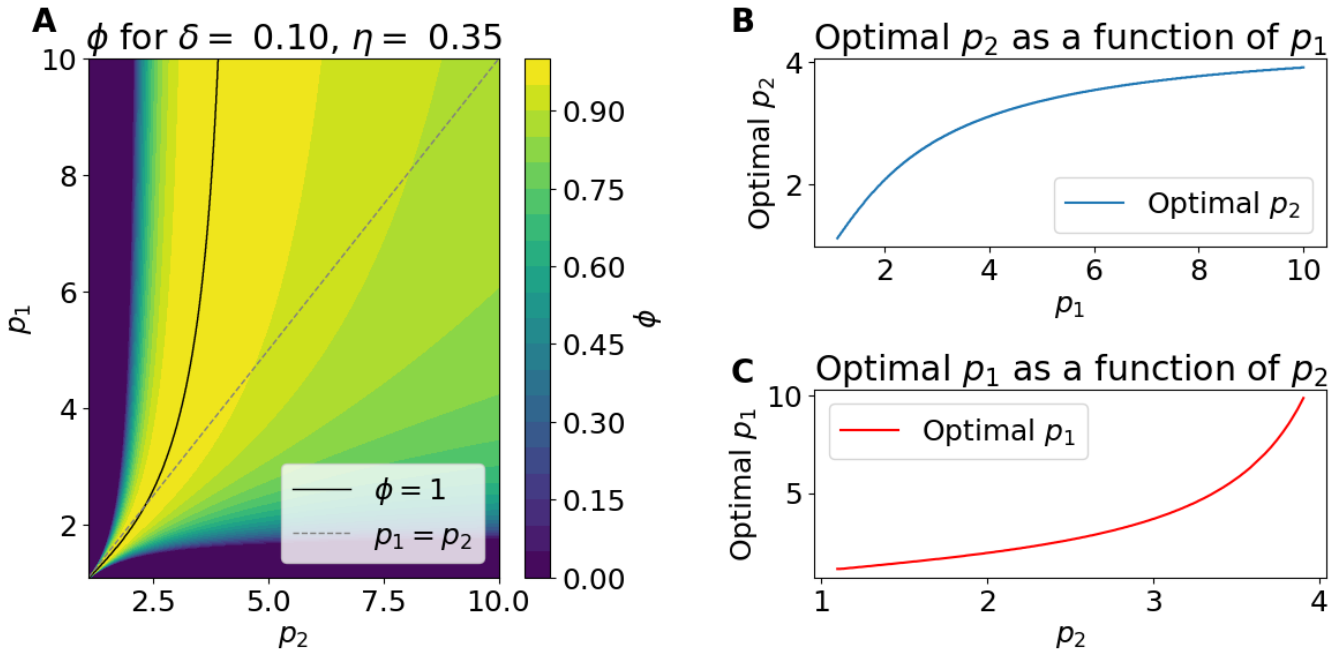

Fig. S4. The dependence of the coexistence ratio, ϕ on p_1 and p_2, with $\delta = 0.1$ and $\eta = 0.35$. (A) Contour plot of ϕ as a function of p_1 and p_2. The black solid line indicates the level curve $\phi = 1$, while the dashed grey line represents $p_1 = p_2$. (B) The optimal value of p_2 as a function of p_1. (C) The optimal value of p_1 as a function of p_2, with data points where $p_1 < 10$ highlighted.

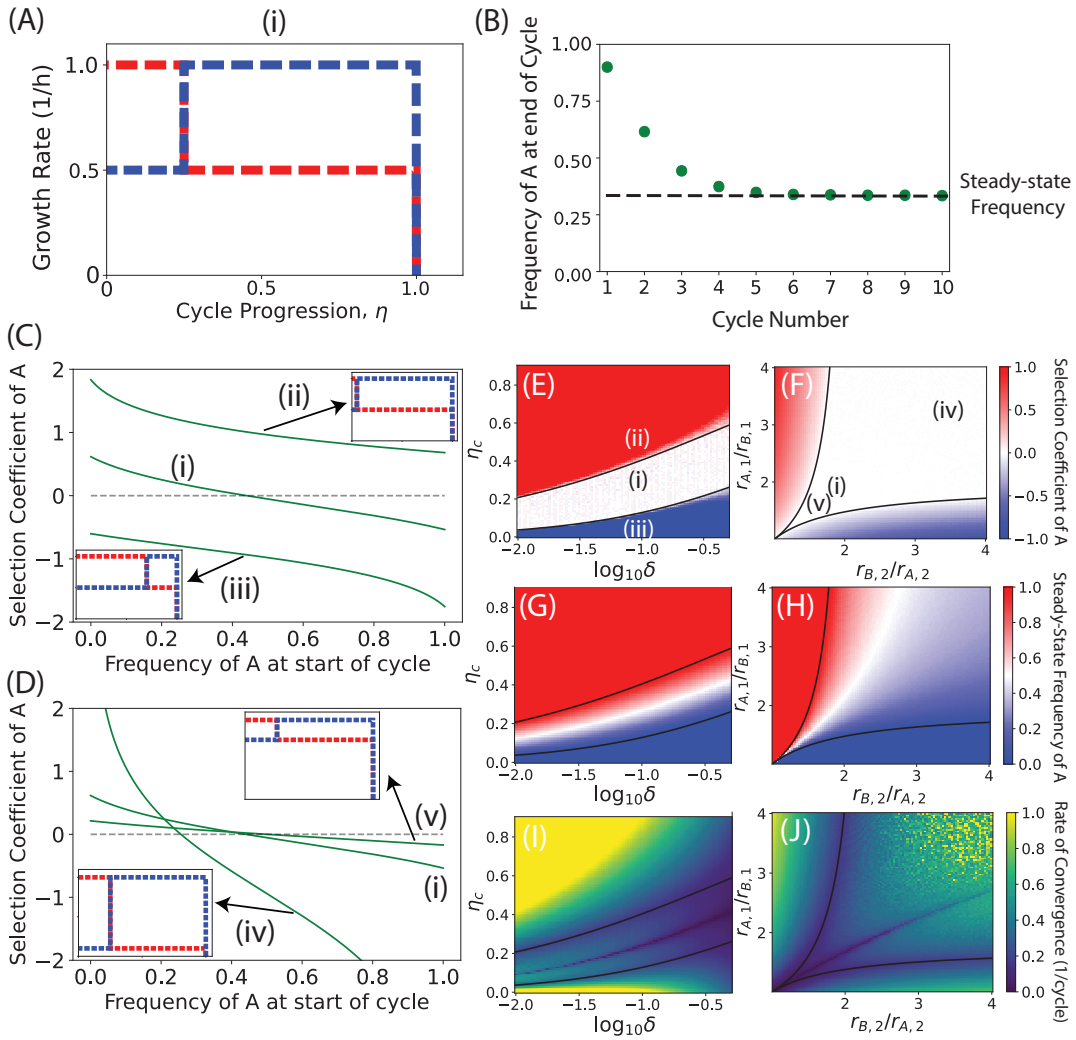

Fig. S5. Partitioning of growth rates reveals quality of coexistence. Features from growth rate dependences on η can be understood by considering perturbations to a piece-wise linear growth rate dependence of two species as shown in (A) and hereby denoted by (i). For all parameters, the coculture eventually arrives at a steady-cycle frequency at the end of the cycle that does not change in subsequent cycles as shown in (B). All results indicated below are for the steady cycle. (C,D) The variation of selection coefficient of A with initial frequency of A for different growth rate dependences (shown in insets and labeled). If the selection coefficient is not 0 for any initial frequency, the two species will not coexist. The effect of the perturbations can be understood more systematically in phase plots where either the environment (in panels E,G,I) or the physiology (in panels F,H,J) of the two species is varied while holding all other parameters constant.

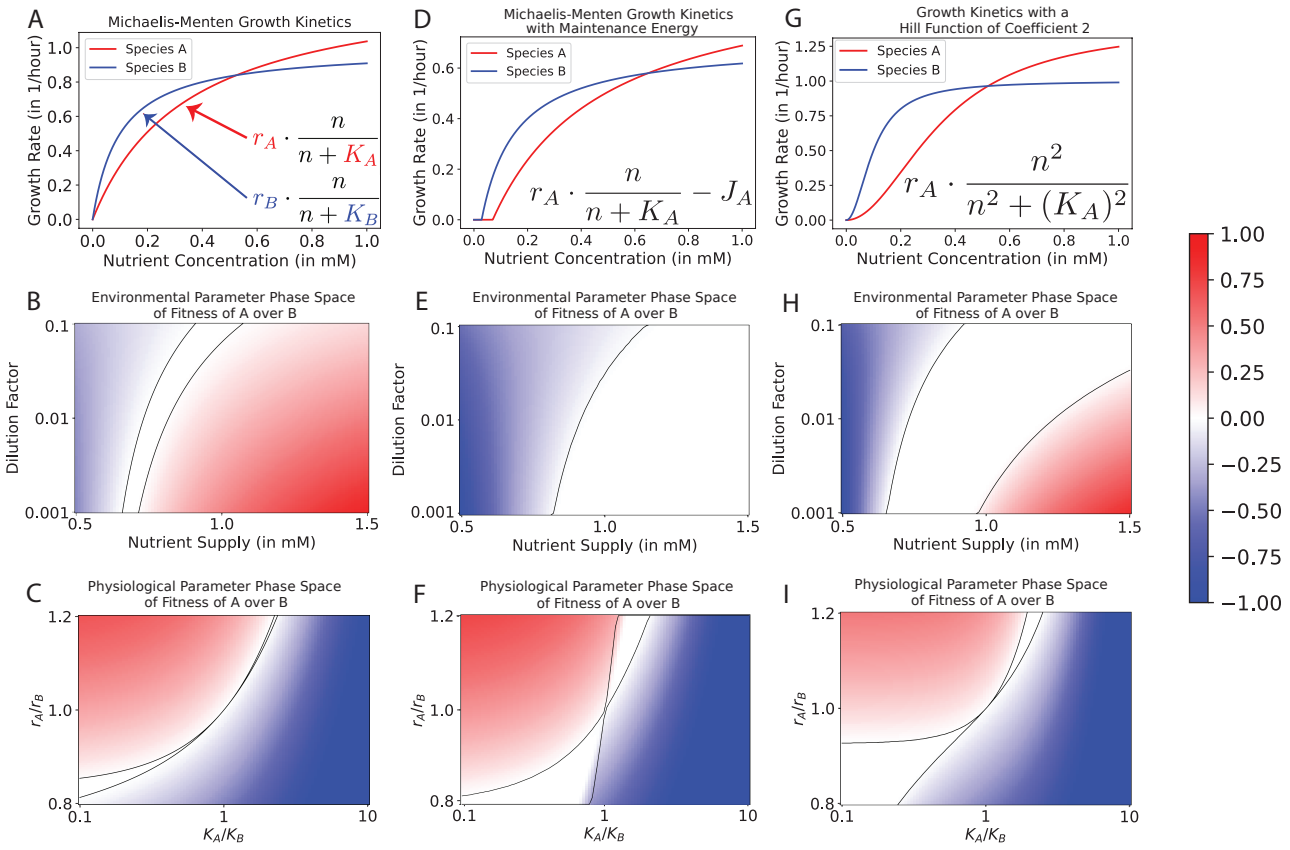

Fig. S6. Biologically-motivated modifications to the Monod growth relation enlarge the coexistence region of phase space. A. Plot showing the standard Monod Growth relation for the dependence of the growth rate on the nutrient concentration of the medium. Two species with different constants describing the growth rates (r_i and K_i) are shown and labeled as Species A and B. **B, E, and H**. Plot showing the fitness of species A over species B over one cycle after 100 cycles (common colorbar shown to the right) for different values of r_A/r_B and K_A/K_B for the respective growth functions of each row. The black lines indicate the boundaries of the analytically determined phase boundaries of coexistence. **B**. Plot showing the fitness of species A over species B over one cycle after 100 cycles (common colorbar shown to the right) for different values of environmental parameters (the nutrient supplied at the beginning of each growth cycle and the dilution factor). The black lines indicate the boundaries of the analytically determined phase boundaries of coexistence. **C**. Plot showing the fitness of species A over species B over one cycle after 100 cycles (common colorbar shown to the right) for different values of physiological parameters of species A, shown as ratios r_A/r_B of the two growth rates and K_A/K_B of the two saturation constant. The black lines indicate the boundaries of the analytically determined phase boundaries of coexistence.

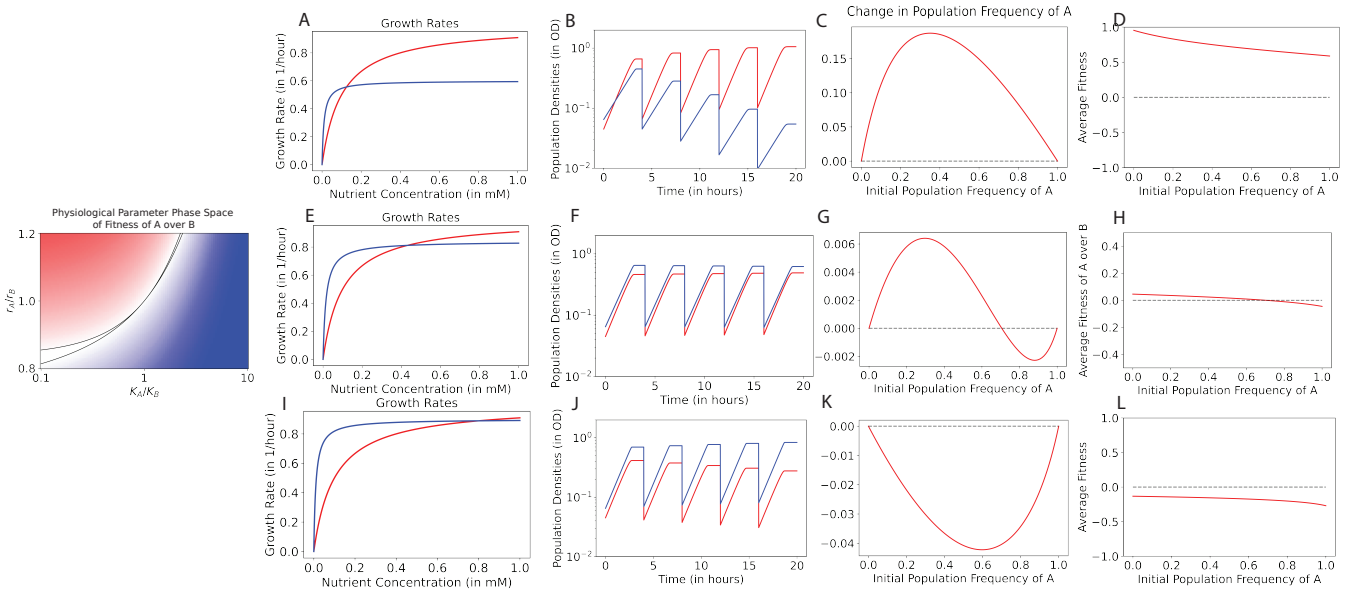

Fig. S7. Assembly of complex communities can be understood by the mutual invasibility criterion for coexistence. A. The growth functions of two species in competition (either of the species can be replaced by a community with the growth rate indicating the growth rate of the entire community, averaged by the frequency of each member of the community). This is determined entirely by the physiological parameters of the two strains. **B.** The ratios of the two growth rates indicate the differential fitness within the cycle. **C.** The differential fitness needs to be weighted by a resource consumption kernel, given by $\omega(s)$ which is a function of the environmental variables, s_0 and δ. If the integral of $r_A(s)/r_B(s)$ curve is ≥ 1, Species A can invade the monoculture of B, and similarly for A. **D.** Iterative flow maps for both Species A and species showing that if both monocultures are invadible, then one fixed point must exist. The invasibility criteria allows one to infer the existence of a coexistence fixed point. If either monoculture is invadable, the trivial fixed point of that monoculture is unstable. As shown in the text, only one non-trivial fixed point can exist.

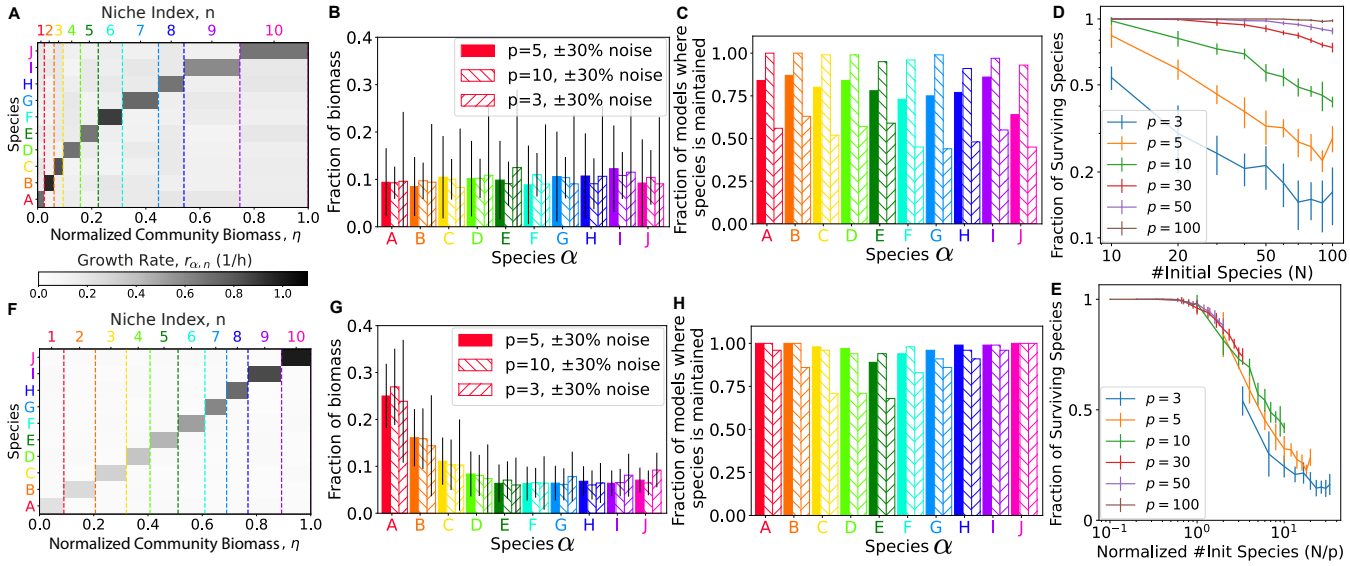

Fig. S8. Impact of disorder and relative changes in growth rate across niches on coexistence (A) Model with exponential niche width, with the value of growth rate for each diagonal entry (i.e., during the preferred niche) assigned randomly within a range of r_+, each off-diagonal entry (non-preferred niches) assigned randomly within a range of r_-. (B) The abundance of each species at the end of the stable cycle, obtained for the model parameters indicated, with $p \equiv r_+/r_-$ being the growth preference. The black lines indicate the standard deviation. (C) The fraction of models where each species is maintained, for the same set of parameters as those indicated in the legend of panel B. (D, E) Abundance of the surviving species for different number of niches N and different growth preferences. Panels F, G, H are the same as panels A, B, C, except that niche widths are fixed to a constant, but the growth preference r_+/r_- is varied using Eq. S134

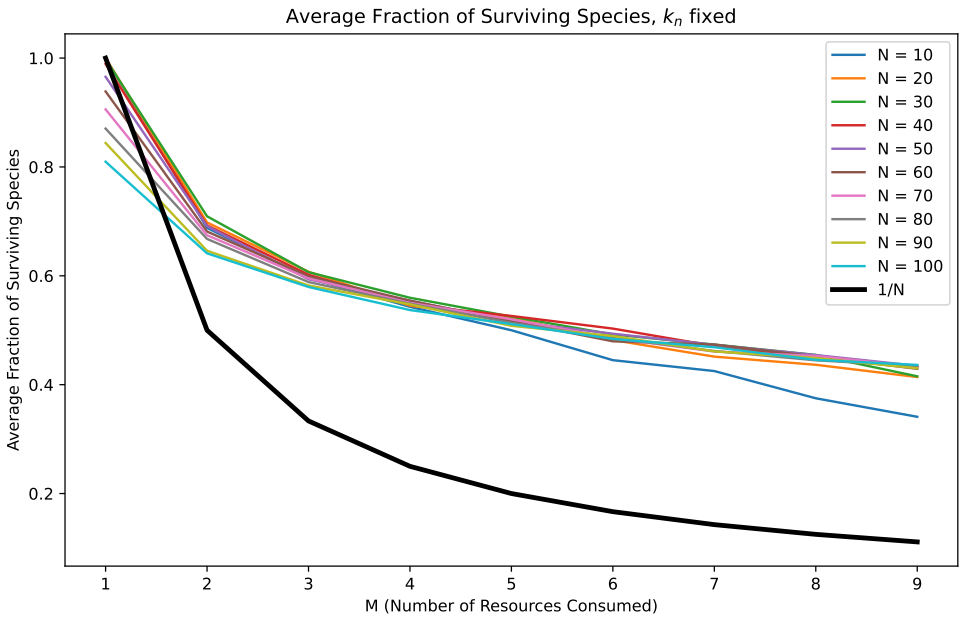

Fig. S9. Average Fraction of Surviving Species with $K_n = M$: The plot shows the average fraction of surviving species in a chemostat model where the number of resources consumed per species (K_n) is held constant. The survival fractions are plotted against varying numbers of resources consumed per species (M). Each line represents a different total number of species/resources (N). The solid black line is $1/M$.

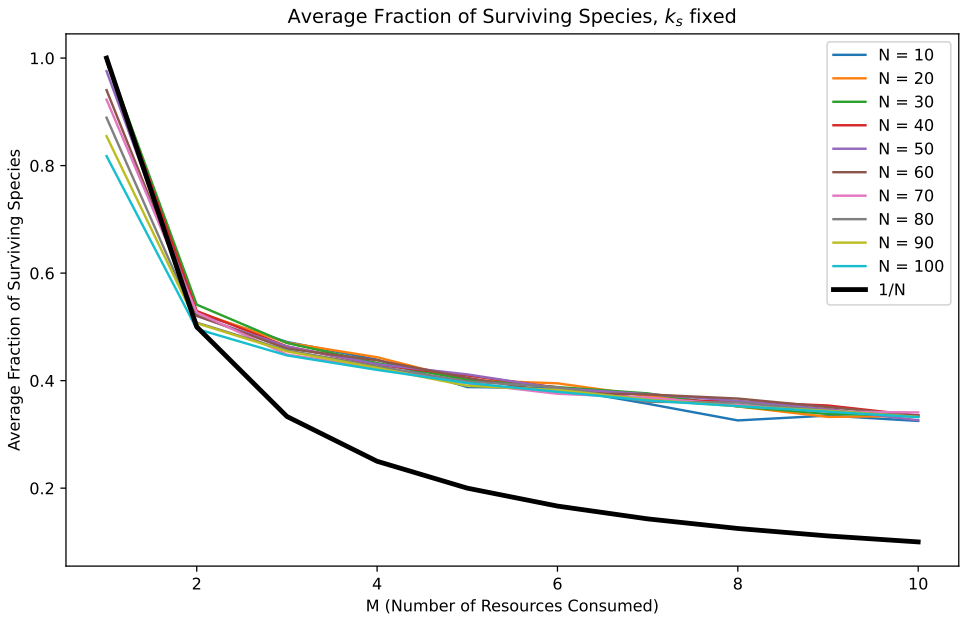

Fig. S10. Average Fraction of Surviving Species with $K_s = M$: The plot shows the survival fractions of species under the condition where the number of species consuming each resource (K_s) is constant. The plot shows how species survival varies with the change in the number of resources consumed per species (M). Different lines correspond to different total numbers of species/resources (N). The solid black line is $1/M$.

S2. Supplementary Text

A. Context on the Competitive Exclusion Principle. The Competitive Exclusion Principle (CEP) states that complete competitors cannot coexist (1). The statement originates with Volterra who used a mathematical model to demonstrate that two species whose growth is limited by the same resource cannot coexist indefinitely (2). This idea was further explored, developed, and disseminated by Lotka (3), Gause (4, 5), and Hutchinson (6). Subsequent theoretical work by MacArthur, Levins, and others (7–10) extended the CEP to state that, in general, there can be no more species than resources.

The CEP is also closely tied to the notion of an ecological niche (11, 12) and is alternatively stated as "No two species can indefinitely continue to occupy the same ecological nich" (13). Levin showed that two species cannot occupy a niche (defined as the hypervolume where the dimensions are environmental conditions and resources, following Hutchinson's definition (6)) unless their limiting factors (for example, nutrients) differ and are independent (14). This echoes MacArthur when he says that the proper statement of the CEP is that "species divide up the resources of a community in such a way that each species is limited by a different factor." (15). We must note that this holds for both biotic and abiotic factors (2, 7, 9, 14).

All the attempts described above contained the assumption that the specific growth rates of the competing species are linear functions of resource or factor densities (16). Further, most attempts (with the exception of Levin (14)) only considered coexistence at fixed densities. In fact, it can be shown that coexistence at fixed densities is limited by the number of resources the species can grow on (16), regardless of the form of the growth rates. When both these constraints are simultaneously relaxed, many species can coexist on a few biotic resources (16–18). A key result was provided by Levins who showed that the number of effective resources is the number of original resources plus the number of distinct non-linearities in the system (19).

Constructive examples rely on the periodic solutions of the Lotka-Volterra model (2) and different points of saturation in the non-linearities of the specific growth rates (we note that nonlinear saturating functional responses are more biologically accurate than linear growth rates (20)). For the case of abiotic resources, Smale showed that that the ordinary differential equation commonly used to describe competing species are compatible with any dynamical behavior provided the number of species is greater than three (21). Following this, systems have been constructed that have periodic orbits (22) with more than three species. Even chaotic behavior has been observed for the case of essential nutrients (23). However, such constructed examples require a large number of species and/or nutrients, need to be carefully constructed, and there is no evidence that they occur naturally. Concurrently, in the 1970s, the importance of non-equilibrium interactions of competing populations in establishing species diversity was emphasized in several investigations (24) (See Chapter 15 of (25)).

B. Example mappings between mechanistic models and step-wise growth. Here we provide some examples of mechanistic models that map on to the Community State Model (in the general formulation of an eco-coordinate). Please note that these are merely examples to illustrate how the CSM might come about rather than a comprehensive mechanistic justification of the CSM. In general, the CSM is a phenomenological model where, in most realistic cases, the parameters (particularly, the relationship between growth rate of each species and the community biomass, and the transition points between different community states) must be determined empirically rather than through mechanistic construction.

B.1. Base Model. We first describe the base model for the growth step of the growth-dilution cycle, and below we will map different consumer-resource models to the base model mathematically.

We take ρ_A to be the population of Species A, ρ_B to be the population of Species B, and η to be the eco-coordinate.

$$\dot{\rho_A} = r_A(\eta) \cdot \rho_A, \tag{S1}$$

where $r_A(\eta) = r_{A,1}$ when $\eta < \eta_k$ and $r_A(s) = r_{A,2}$ when $\eta > \eta_k$.

$$\dot{\rho_B} = r_B(\eta) \cdot \rho_B, \tag{S2}$$

where $r_B(\eta) = r_{B,1}$ when $\eta < \eta_k$ and $r_B(s) = r_{B,2}$ when $\eta > \eta_k$.

$$\dot{\eta} = r_A(\eta) \cdot \rho_A + r_B(\eta) \cdot \rho_B. \tag{S3}$$

η starts at 0 and ends at 1. In general, $r_A(s)$ and $r_B(s)$ need not be piece-wise constant, but can be a linear interpolation if continuity of $r(s)$ is important, and indeed any curve if specific properties are necessary.

B.2. Step-Wise Growth. We take N_A to be the population of Species A, N_B to be the population of Species B, and s to be the nutrient. The consumer resource model is given by

$$\dot{N_A} = r_A(s)N_A, \tag{S4}$$

where $r_A(s) = r_{A,1}$ when $s > s_k$ and $r_A(s) = r_{A,2}$ when $s < s_k$.

$$\dot{N_B} = r_B(s)N_B, \tag{S5}$$

where $r_B(s) = r_{B,1}$ when $s > s_k$ and $r_B(s) = r_{B,2}$ when $s < s_k$.

$$\dot{s} = -r_A(s)N_A/Y_A - r_B(s)N_B/Y_B. \tag{S6}$$

The environmental variables are given by s_0, the total amount of nutrient supplied at first, and δ, the dilution fold.
We redefine the variables as follows:

$$\eta \equiv 1 - \frac{s}{s_0} \tag{S7}$$

$$\eta_k \equiv 1 - \frac{s_k}{s_0} \tag{S8}$$

$$\rho_A \equiv \frac{N_A}{s_0 \cdot Y_A} \tag{S9}$$

$$\rho_B \equiv \frac{N_B}{s_0 \cdot Y_B} \tag{S10}$$

This creates an exact equivalence to the base model.

B.3. Diauxie. Here we discuss the case of diauxic growth for two species with the same resource preferences. For the case of heterogenous resource preferences, please refer to (26, 27).
We take N_A to be the population of Species A, N_B to be the population of Species B, s_1 to be the concentration of the first nutrient consumed and s_2 to be the concentration of the second nutrient consumed. The consumer resource model is given by

$$\dot{N_A} = r_{A,1}(s_1)N_A + r_{A,2}(s_1, s_2)N_A, \tag{S11}$$

where $r_{A,1}(s_1) = r_{A,1} \cdot \Theta(s_1)$ and $r_{A,2}(s_1, s_2) = r_{A,2} \cdot \Theta(-s_1) \cdot \Theta(s_2)$. Θ is the Heaviside step-function

$$\dot{N_B} = r_{B,1}(s_1)N_B + r_{B,2}(s_1, s_2)N_B, \tag{S12}$$

where $r_{B,1}(s_1) = r_{B,1} \cdot \Theta(s_1)$ and $r_{B,2}(s_1, s_2) = r_{B,2} \cdot \Theta(-s_1) \cdot \Theta(s_2)$.

$$\dot{s_1} = -r_{A,1}(s_1)\frac{N_A}{Y_A \cdot Y_1} - r_{B,1}(s_1, s_2)\frac{N_B}{Y_B \cdot Y_1}. \tag{S13}$$

$$\dot{s_2} = -r_{A,2}(s_2)\frac{N_A}{Y_A \cdot Y_2} - r_{B,2}(s_1, s_2)\frac{N_B}{Y_B \cdot Y_2}. \tag{S14}$$

The environmental variables are given by $s_1^{(0)}$ and $s_2^{(0)}$, the total amount of nutrients supplied at first, and δ, the dilution fold.
We redefine the variables as follows:

$$\eta \equiv \begin{cases} 1 - \frac{Y_1 \cdot s_1 + Y_2 \cdot s_2^{(0)}}{(Y_1 \cdot s_1^{(0)} + Y_2 \cdot s_2^{(0)})}, s_1 > 0 \\ 1 - \frac{Y_2 \cdot s_2}{(Y_1 \cdot s_1^{(0)} + Y_2 \cdot s_2^{(0)})}, s_1 = 0 \end{cases} \tag{S15}$$

$$\eta_k \equiv \frac{Y_1 \cdot s_1^{(0)}}{(Y_1 \cdot s_1^{(0)} + Y_2 \cdot s_2^{(0)})} \tag{S16}$$

$$\rho_A \equiv \frac{N_A}{Y_A \cdot (Y_1 \cdot s_1^{(0)} + Y_2 \cdot s_2^{(0)})} \tag{S17}$$

$$\rho_B \equiv \frac{N_B}{Y_B \cdot (Y_1 \cdot s_1^{(0)} + Y_2 \cdot s_2^{(0)})} \tag{S18}$$

This gives us that:

$$\dot{\rho_A} = r_A(\eta)\rho_A, \tag{S19}$$

where $r_A(\eta) = r_{A,1} \cdot \Theta(\eta_k - \eta)$ and $r_A(\eta) = r_{A,2} \cdot \Theta(\eta - \eta_k) \cdot \Theta(1 - \eta)$.

$$\dot{\rho_B} = r_B(\eta)\rho_B, \tag{S20}$$

where $r_B(\eta) = r_{B,1} \cdot \Theta(\eta_k - \eta)$ and $r_B(\eta) = r_{B,2} \cdot \Theta(\eta - \eta_k) \cdot \Theta(1 - \eta)$.

$$\dot{\eta} = r_A(\eta)\rho_A + r_B(\eta)\rho_B. \tag{S21}$$

This creates an exact equivalence to the base model.

B.4. Oxygen Depletion. We take N_A to be the population of Species A, N_B to be the population of Species B, s to be the concentration of the nutrient, and x to be the concentration of oxygen. The consumer resource model is given by

$$\dot{N_A} = r_A(s,x)N_A, \tag{S22}$$

where $r_A(s,x) = r_{A,1} \cdot \Theta(x) + r_{A,2} \cdot \Theta(-x) \cdot \Theta(s)$.

$$\dot{N_B} = r_B(s,x)N_B, \tag{S23}$$

where $r_B(s,x) = r_{B,1} \cdot \Theta(x) + r_{B,2} \cdot \Theta(-x) \cdot \Theta(s)$.

$$\dot{s} = -r_A(s,x)N_A/Y_A - r_B(s,x)N_B/Y_B. \tag{S24}$$

$$\dot{x} = (-r_{A,1} \cdot \frac{N_A}{Y_A \cdot Y_x} - r_{B,1} \cdot \frac{N_B}{Y_B \cdot Y_x})\Theta(x). \tag{S25}$$

The environmental variables are given by s_0 and x_0, the total amount of nutrient and oxygen supplied at first, and δ, the dilution fold. For oxygen to deplete first, we need $x_0 < s_0 \cdot Y_x$
We redefine the variables as follows:

$$\eta \equiv 1 - \frac{s}{s_0} \tag{S26}$$

$$\eta_k \equiv 1 - \frac{x_0}{s_0 \cdot Y_x} \tag{S27}$$

$$\rho_A \equiv \frac{N_A}{s_0 \cdot Y_A} \tag{S28}$$

$$\rho_B \equiv \frac{N_B}{s_0 \cdot Y_B} \tag{S29}$$

This creates an exact equivalence to the base model.

B.5. Quorum Sensing. We take N_A to be the population of Species A, N_B to be the population of Species B, s to be the concentration of the nutrient, and q to be the concentration of autoinducer. The consumer resource model is given by

$$\dot{N_A} = r_A(s,x)N_A, \tag{S30}$$

where $r_A(s,x) = r_{A,1}$ when $q < q_k$, $r_{A,2}$ when $q > q_k$, and 0 when $s = 0$.

$$\dot{N_B} = r_B(s,x)N_B, \tag{S31}$$

where $r_B(s,x) = r_{B,1}$ when $q < q_k$, $r_{B,2}$ when $q > q_k$, and 0 when $s = 0$.

$$\dot{s} = -r_A(s,x)N_A/Y_A - r_B(s,x)N_B/Y_B. \tag{S32}$$

$$\dot{q} = r_{A,1} \cdot \frac{N_A}{Y_A \cdot Y_q} + r_{B,1} \cdot \frac{N_B}{Y_B \cdot Y_q}. \tag{S33}$$

The environmental variables are given by s_0, the total amount of nutrient supplied at first, and δ, the dilution fold. For the autoinducer to accumulate first, we need $q_k < s_0 \cdot Y_q$
We redefine the variables as follows:

$$\eta \equiv 1 - \frac{s}{s_0} \tag{S34}$$

$$\eta_k \equiv 1 - \frac{q_k}{s_0 \cdot Y_q} \tag{S35}$$

$$\rho_A \equiv \frac{N_A}{s_0 \cdot Y_A} \tag{S36}$$

$$\rho_B \equiv \frac{N_B}{s_0 \cdot Y_B} \tag{S37}$$

This creates an exact equivalence to the base model.

B.6. Acid Stress. We take N_A to be the population of Species A, N_B to be the population of Species B, s to be the concentration of the nutrient, x to be the concentration of acid, and p to be the concentration of pyruvate. The consumer resource model is given by

$$\dot{N_A} = r_A(s,x,p) \cdot N_A, \tag{S38}$$

where $r_A(s,x) = r_{A,1}$ when $x < x_c$, $r_{A,2}$ when $x > x_c$, and 0 when $s = 0$.

$$\dot{N_B} = r_B(s,x,p) \cdot N_B, \tag{S39}$$

where $r_B(s,x) = r_{B,1}$ when $x < x_c$, $r_{B,2}$ when $x > x_c$, and 0 when $s = 0$.

$$\dot{s} = -r_A \cdot \frac{N_A}{Y_A \cdot Y_s}. \tag{S40}$$

$$\dot{x} = r_A \cdot \frac{N_A}{Y_A \cdot Y_x} \cdot f_x - r_B \cdot \frac{N_B}{Y_B \cdot Y_x}. \tag{S41}$$

$$\dot{p} = r_A \cdot \frac{N_A}{Y_A \cdot Y_p} \cdot f_p - r_B \cdot \frac{N_B}{Y_B \cdot Y_p}. \tag{S42}$$

such that $f_x + f_p < 1$ and the fractions of the nutrient consumed that Species A converts to acid and pyruvate. The environmental variables are given by s_0, the total amount of nutrient supplied at first, and δ, the dilution fold. We redefine the variables as follows:

$$\eta \equiv 1 - \frac{Y_s \cdot s + Y_x \cdot x + Y_p \cdot p}{Y_s \cdot s_0} \tag{S43}$$

$$\rho_A \equiv \frac{N_A}{s_0 \cdot Y_A} \tag{S44}$$

$$\rho_B \equiv \frac{N_B}{s_0 \cdot Y_B} \tag{S45}$$

All that remains to resolve is the question of η_k since in the actual system, it is only given by the acetate concentration, x_c. However, we can take x_c to be a function of η if $\eta(t) \propto x(t)$:

$$\eta(x = x_c) \equiv 1 - \frac{Y_s \cdot s(x_c) + Y_x \cdot x_c}{Y_s \cdot s_0} \tag{S46}$$

In reality,

$$\eta(t) = N_A \cdot (\exp(r_{A,1} \cdot t) - 1) \cdot \frac{1}{Y_A \cdot Y_s} \tag{S47}$$

$$x(t) = N_A \cdot (\exp(r_{A,1} \cdot t) - 1) \cdot \frac{1}{Y_A \cdot Y_x} - N_B \cdot (\exp(r_{B,1} \cdot t) - 1) \cdot \frac{1}{Y_B \cdot Y_x} \tag{S48}$$

$$= \eta(t) \cdot \frac{Y_s}{Y_x} - \frac{N_B}{Y_B \cdot Y_x} \cdot (\exp(r_{B,1} \cdot t) - 1) \tag{S49}$$

$$= \eta(t) \cdot \frac{Y_s}{Y_x} - \frac{N_B}{Y_B \cdot Y_x} \cdot \left(\frac{Y_A \cdot Y_s \cdot \eta(t)}{N_A} \right)^{r_{B,1}/r_{A,1}} \tag{S50}$$

Thus, $\eta(t) \propto x(t)$ if $r_{B,1} \ll r_{A,1}$ (or $N_B \ll N_A$). This creates an exact equivalence to the base model.

C. Rescaling. Here, we discuss the rescaling of the time spent in each phase/niche and the transition points in the piece-wise linear models discussed in the paper. The rescaling of the transition points amounts to a redefinition of the units with $\rho_{\text{tot}}^{\max}$ declared to be 1, with an appropriate normalization of all transition points by $\rho_{\text{tot}}^{\max}$. For the many species model, we additionally define a parameter, $\eta \equiv (\rho_{\text{tot}}/\rho_{\text{tot}}^{\max} - \delta)/(1 - \delta)$, for simplification of the results such that the cycle starts at $\eta = 0$ and ends at $\eta = 1$. For rescaling the time spent in each phase, we first note that in the limit of large time between dilution events, there is no activity once the system reaches the total biomass density of the system reaches $\rho_{\text{tot}}^{\max}$. Thus, we may ignore the timescales associated with dilution. Next, we consider the dynamics within niche/phase, n:

$$\frac{d}{dt}\rho_\alpha^{(j)} = r_{\alpha,n} \cdot \rho_\alpha^{(j)}(t) \qquad \text{for } \eta_{n-1} \le \eta \le \eta_{n-1}. \tag{S51}$$

The dynamics in this interval is essentially independent of every other phase as the system is autonomous in time. Thus we may define, for example, the dimensionless time, $\tau_n \equiv t \cdot \langle \alpha r_{\alpha,n} \rangle_{\alpha \neq \alpha(n)}$. Hence, rescaling t by τ_n, we obtain that the dynamics of $\rho_\alpha^{(j)}$ in niche n given by

$$\frac{d}{d\tau_n}\rho_\alpha^{(j)} = \frac{r_{\alpha,n}}{\langle \alpha r_{\alpha,n} \rangle_{\alpha \neq \alpha(n)}} \cdot \rho_\alpha^{(j)}(t) \qquad \text{for } \eta_{n-1} \le \eta \le \eta_{n-1}. \tag{S52}$$

This allows us to define $p_n \equiv \frac{r_{\alpha,n}}{\langle \alpha r_{\alpha,n} \rangle_{\alpha \neq \alpha(n)}}$. Thus, in the cases without noise described in this manuscript, each niche is effectively described by one number: the domination of the fast-growing species in niche n over the slow-growing species.

D. Mathematical Results for the Simple Toy Model. Though we have shown that two species may coexist in growth-dilution cycles, understanding the dynamics of the co-culture system mathematically can be significantly difficult because of the non-linear growth rates involved. To simplify the system, we consider a piece-wise linear approximation of the system (as shown in Fig. 3A). In this Toy Model, we take Species A to grow at a constant rate $r_{A,1}$ and Species B at $r_{B,1}$ while biomass values are above a threshold s_k (we call this the first phase and call the time taken to complete it τ_1). And in the 2nd phase (biomass from 0 to η_k, taking time τ_2), we take Species A to grow at $r_{A,2}$ and Species B at $r_{B,2}$ (this toy model is described in Fig. 3A). When biomass reaches $\rho_{\text{tot}}^{\max}$, we assume that both species stop growing.

If two species coexist in such a system, it implies that the net growth rate is the same over the steady-state cycle, i.e.,

$$r_{A,1}\tau_1 + r_{A,2}\tau_2 = r_{B,1}\tau_1 + r_{B,2}\tau_2 = -\log\delta. \tag{S53}$$

We note that as long as there is a trade-off in the growth rates (such that neither species is growing faster than the other species at all biomass values), there exists a positive τ_1 and τ_2 that can solve Eq. **S53**. However, Eq. **S53** is also coupled with a set of equations describing the biomass increase that feature the populations of both species, $\rho_A(0)$ and $\rho_B(0)$, at the beginning of the cycle:

$$\rho_{\text{tot}}^{c} - \delta\cdot\rho_{\text{tot}}^{\max} = (e^{r_{A,1}\tau_1}-1)\rho_A(0) + (e^{r_{B,1}\tau_1}-1)\rho_B(0), \tag{S54}$$

$$\rho_{\text{tot}}^{\max} - \rho_{\text{tot}}^{c} = (e^{r_{A,2}\tau_2}-1)e^{r_{A,1}\tau_1}\rho_A(0) + (e^{r_{B,2}\tau_2}-1)e^{r_{B,1}\tau_1}\rho_B(0). \tag{S55}$$

We obtain the equations above as the total amount of biomass produced by both species must be $\rho_{\text{tot}}^{c} - \delta\cdot\rho_{\text{tot}}^{\max}$ in the first phase (as the co-culture starts with biomass of $\delta\cdot\rho_{\text{tot}}^{\max}$ after dilution by a factor of δ from the maximal biomass value of ρ_{tot}, and $\rho_{\text{tot}}^{\max} - \rho_{\text{tot}}^{c}$ in the second phase. The solution to Eq. **S54**-Eq. **S55**, however, may not yield a viable positive solution for $\rho_A(0)$ and $\rho_B(0)$. For viable solutions, we require that the two species must necessarily engage in resource sharing in the steady-state cycle described by τ_1 and τ_2 that solve Eq. **S53**, as otherwise they would not be able to accumulate all of the biomass by themselves. If any resources remain unconsumed in a monoculture (say of Species A), a very small population of Species B can consume the remaining resources and grow more than the dilution fold. Eventually, the very small population grows larger and the factor of growth decreases until both species grow at the dilution fold.

Thus, to get $\rho_A(0) > 0$, we must have (assuming $r_{A,1} > r_{B,1} > 0,\ r_{B,2} > r_{A,2} > 0$):

$$\rho_A(0) > 0 \iff \underbrace{\rho_{\text{tot}}^{c} - \delta\cdot\rho_{\text{tot}}^{\max}}_{\text{Biomass produced in phase 1}} > \underbrace{(e^{r_{B,1}\tau_1}-1)}_{\text{Net Growth of B in } \tau_1} \cdot \underbrace{\delta\cdot\rho_{\text{tot}}^{\max}}_{\text{Max population of B at start of phase 1}} \tag{S56}$$

And similarly, requiring that $\rho_B > 0$, we have that

$$\rho_B(0) > 0 \iff \underbrace{\rho_{\text{tot}}^{c} - \delta\cdot\rho_{\text{tot}}^{\max}}_{\text{Biomass produced in phase 1}} < \underbrace{(e^{r_{A,1}\tau_1}-1)}_{\text{Net Growth of A in } \tau_1} \cdot \underbrace{\delta\cdot\rho_{\text{tot}}^{\max}}_{\text{Max population of A at start of phase 1}} \tag{S57}$$

Or by looking at phase 2,

$$\rho_B(0) > 0 \iff \underbrace{\rho_{\text{tot}}^{\max} - \rho_{\text{tot}}^{c}}_{\text{Biomass produced in phase 2}} > \underbrace{(e^{r_{A,2}\tau_2}-1)}_{\text{Net Growth of A in } \tau_2} \cdot \underbrace{\delta\cdot\rho_{\text{tot}}^{\max}\cdot e^{r_{A,1}\tau_1}}_{\text{Max population of A at start of phase 2}} \tag{S58}$$

But Eq. **S56** and Eq. **S57** are just saying that resource sharing must be possible for the necessary τ_1 as we require that the resources consumed by the co-culture in τ_1 be greater than the resources that a monoculture of B would have consumed, and less what a monoculture of A would have consumed (we need the second requirement as otherwise you do reach phase 2 before τ_1, and thus you cannot have coexistence). Similarly, we get that the resources in phase 2 should be more than the monoculture of A could consume on its own. In fact, if we add up the two conditions, we get that you need resource sharing of total biomass must be possible). We note that both Eq. **S56** and Eq. **S57** are not necessarily true (trivially, we can move $\rho_{\text{tot}}^{\max} - \rho_{\text{tot}}^{c}$ so that either Eq. **S56** or Eq. **S57** are not satisfied as the RHS is independent of $\rho_{\text{tot}}^{\max} - \rho_{\text{tot}}^{c}$). Thus, only certain monocultures permit resource sharing. Further, we note that the ones that do, are stable since if there's resources that could be consumed that a monoculture cannot consume, it allows for invasion that can grow in a time period given by matrix inversion.

We now solve for $\rho_A(0)$ and $\rho_B(0)$ that satisfy Eq. **S53-S55**. First, from Eq. **S53**, we obtain,

$$\tau_1 = -\log\delta\cdot\left(\frac{r_{A,2}-r_{B,2}}{r_{B,1}\cdot r_{A,2} - r_{B,2}\cdot r_{A,1}}\right) \tag{S59}$$

$$= \log(1/\delta)\cdot\frac{1}{r_{B,1}}\left(\frac{p_2-1}{p_1\cdot p_2 - 1}\right). \tag{S60}$$

And similarly, we obtain

$$\tau_2 = -\log\delta\cdot\left(\frac{r_{A,1}-r_{B,1}}{r_{A,1}\cdot r_{B,2} - r_{A,2}\cdot r_{B,1}}\right) = \log(1/\delta)\cdot\frac{1}{r_{A,2}}\left(\frac{p_1-1}{p_1\cdot p_2 - 1}\right). \tag{S61}$$

We note that this value is independent of ρ^c_{tot} and $\rho^{\max}_{\text{tot}}$. We first note that Eq. S57 and Eq. S58 are now given in terms of model parameters by

$$\rho_A(0) > 0 \iff \rho^c_{\text{tot}} - \delta \cdot \rho^{\max}_{\text{tot}} > \left(\delta^{\frac{1-p_2}{p_1 p_2 - 1}} - 1\right) \cdot \delta \cdot \rho^{\max}_{\text{tot}} \tag{S62}$$

$$\iff \eta_c > \delta^{\frac{p_1-1}{p_1 - 1/p_2}}, \tag{S63}$$

where $\eta_c \equiv \rho^c_{\text{tot}}/\rho^{\max}_{\text{tot}}$. Similarly,

$$\rho_B(0) > 0 \iff \rho^c_{\text{tot}} - \delta \cdot \rho^{\max}_{\text{tot}} < \left(\delta^{\frac{p_1 - p_1 p_2}{p_1 p_2 - 1}} - 1\right) \cdot \delta \cdot \rho^{\max}_{\text{tot}} \tag{S64}$$

$$\iff \eta_c < \delta^{\frac{1}{p_2}\frac{p_1-1}{p_1 - 1/p_2}}. \tag{S65}$$

This gives us that there is coexistence if

$$\delta^{\frac{p_1-1}{p_1-1/p_2}} < \eta_c < \delta^{\frac{1}{p_2}\frac{p_1-1}{p_1-1/p_2}}, \tag{S66}$$

$$1 > \frac{p_1 - 1/p_2}{p_1 - 1}\frac{\log \eta_c}{\log \delta} > \frac{1}{p_2}. \tag{S67}$$

which is equivalent to one obtained by the Mutual Invasibility Criterion.

To obtain the steady-state values of $\rho_A(0)$ and $\rho_B(0)$, which we denote with ρ^*_A and ρ^*_B (note that $\rho^*_A + \rho^*_B = \delta \cdot \rho^{\max}_{\text{tot}}$), we use Eq. S54-S55 to obtain

$$\rho^c_{\text{tot}} - \delta \cdot \rho^{\max}_{\text{tot}} = (e^{r_{A,1}\tau_1} - 1)\rho^*_A + (e^{r_{B,1}\tau_1} - 1)(\delta\rho^{\max}_{\text{tot}} - \rho^*_A) \tag{S68}$$

$$\implies \rho^*_A = \frac{\rho^c_{\text{tot}} - e^{r_{B,1}\tau_1}\delta\rho^{\max}_{\text{tot}}}{e^{r_{A,1}\tau_1} - e^{r_{B,1}\tau_1}} \tag{S69}$$

$$= \min\left(1, \max\left(0, \frac{\eta_c - \delta^{\frac{p_1-1}{p_1-1/p_2}}}{\delta^{\frac{1-p_2}{p_2-1/p_1}} - \delta^{\frac{1-p_2}{p_1 \cdot p_2 - 1}}}\right)\right) \cdot \rho^{\max}_{\text{tot}}, \tag{S70}$$

and similarly,

$$\rho^*_B = \frac{\rho^c_{\text{tot}} - e^{r_{A,1}\tau_1}\delta\rho^{\max}_{\text{tot}}}{e^{r_{B,1}\tau_1} - e^{r_{A,1}\tau_1}} \tag{S71}$$

$$= \min\left(1, \max\left(0, \frac{\delta^{\frac{p_1-1}{p_1 \cdot p_2 - 1}} - \eta_c}{\delta^{\frac{1-p_2}{p_2-1/p_1}} - \delta^{\frac{1-p_2}{p_1 \cdot p_2 - 1}}}\right)\right) \cdot \rho^{\max}_{\text{tot}}. \tag{S72}$$

Thus, while there is a non-trivial dependence on δ, p_1, and p_2, there is a linear dependence on η_c and $\rho^{\max}_{\text{tot}}$. Below, we explore the non-trivial dependence on p_1, and p_2. This analysis also tells us that there can only be one viable non-trivial solution for ρ^*_A and ρ^*_B (in other words, there can only be one non-trivial fixed point for the discrete map given by one growth-dilution cycle). This is why the complete system at steady-state can be understood by studying the trivial fixed points (i.e., the respective monocultures) as if both trivial fixed points are unstable to invasion, the system must have a non-trivial fixed point. Further, we can show that if it exists, the non-trivial fixed point must be stable. Intuitively, this is because if the frequency of Species A is increased, the amount of time it would take for the population to produce all of the allocated biomass in its preferred phase will be shorter, thus harming Species A. Similarly, the amount of time it would take for the population to accumulate all of the biomass in the phase that it is growing slower will be longer, once again harming Species A. Thus, there can only be one stable fixed point in the system.

Eq. S69 and Eq. S72 also provide the values for the coexistence ratio, ϕ:

$$\phi \equiv \frac{4\rho^*_A \cdot \rho^*_B}{(\rho^*_A + \rho^*_B)^2} \tag{S73}$$

$$= \max\left(0, -4 \cdot \frac{\left(\delta^{\frac{p_1-1}{p_1 p_2 - 1}} - \eta_c\right) \cdot \left(\delta^{\frac{p_2(p_1-1)}{p_1 p_2 - 1}} - \eta_c\right)}{\left(\delta^{\frac{p_1-1}{p_1 p_2 - 1}} - \delta^{\frac{p_2(p_1-1)}{p_1 p_2 - 1}}\right)^2}\right). \tag{S74}$$

We now note the limit of ϕ as p_1 or p_2 go to ∞:

$$\phi(p_1 \to \infty) \to \max\left(0, \frac{-4 \cdot \left(\delta^{1/p_2} - \eta_c\right) \cdot (\delta - \eta_c)}{(\delta - \delta^{1/p_2})^2}\right) \tag{S75}$$

$$\phi(p_2 \to \infty) \to \max\left(0, \frac{-4 \cdot \delta^{1/p_1} \cdot (1 - \eta_c) \cdot \left(\delta - \delta^{1/p_1} \cdot \eta_c\right)}{(\delta - \delta^{1/p_1})^2}\right) \tag{S76}$$

While determining the optimal p_1 and p_2 for ϕ can be challenging analytically as it requires solving a transcendental equation, we present some numerical solutions in *Supplementary Fig.* S4.

We note that this method can be extended to many species (say m) and many phases (say k(as well, resulting in the following matrix equations:

$$G \cdot \vec{\tau} = -\log \delta \cdot \vec{1_m} \tag{S77}$$

$$dn_i = \sum_{\alpha}^{m} \left(\exp(G_{\alpha,i}\tau_i) - 1\right) \exp\left(\sum_{j}^{i-1} G_{\alpha,j}\tau_j\right) \rho_\alpha \tag{S78}$$

where G is the growth matrix such that species α and dn_i is the amount of biomass gained in phase i. While it can be difficult to solve this equation as it requires solving a system of transcendental equations of many variables, this approach does tell us that there can be exactly one solution for $\{\rho_\alpha^*\}$. This is because there is an unknown variable for each species (ρ_α^*), and a corresponding equation for each species. While this system of equations for each species features an unknown variable for each phase (τ_i), the equations for resource constraints provide another set of equations for each τ_i (which is the transcendental system of equations). Thus, unless the system of transcendental equations produces a degeneracy for τ_i, there is exactly one $\{\rho_\alpha^*\}$ that solves the system of equations. This result will be rigorously shown for any non-negative function $r_\alpha(\eta)$ below.

E. Self-consistency and stability of the Community State Model. We consider a serial dilution system involving several species such that the growth of a species α during the j^{th} cycle is described by

$$\frac{d}{dt}\rho_\alpha^{(j)} = r_\alpha\left(\vec{S}(t)\right) \cdot \rho_\alpha^{(j)}(t) \qquad \text{for } 0 \le t \le T. \tag{S79}$$

When t reaches the growth period T, all densities are reduced by a common factor $\delta < 1$, i.e.,

$$\rho_\alpha^{(j+1)}(t=0) = \delta \cdot \rho_\alpha^{(j)}(t=T). \tag{S80}$$

E.1. Local Stability Condition. We note that at a fixed point, $\rho_\alpha^{(j+1)}(t=0) = \rho_\alpha^{(j)}(t=0)$. This gives us that:

$$\delta \cdot \rho_\alpha^{(j)}(t=T) = \rho_\alpha^{(j)}(t=0) \tag{S81}$$

$$\implies \delta \cdot \rho_\alpha^{(j)}(t=0) \exp\left(\int_0^T r_\alpha\left(\vec{S}(t)\right) dt\right) = \rho_\alpha^{(j)}(t=0) \tag{S82}$$

$$\implies \log\delta + \int_0^T r_\alpha\left(\vec{S}(t)\right) dt = 0 \tag{S83}$$

E.2. Low-Dimensional Reduction. If the trajectory $\vec{S}(t)$ taken by the system in steady state can be written as a scalar bijective function $\eta(t)$, we can write

$$\implies \int_0^T r_\alpha\left(\eta(t)\right) dt = -\log\delta$$

By changing variables from t to $\eta(t)$

$$\int_{\eta(0)}^{\eta(T)} \frac{r_\alpha(\eta(t))}{d\eta/dt} d\eta = -\log(\delta). \tag{S84}$$

This provides the local stability condition, Eq. **S84** which must hold for all species α at a fixed point.

E.3. Negative Frequency-Dependence of Fitness. First, we assume that η goes from η_0 to $\eta_{\max}$ in every cycle. This is expected if $\dot{\eta}(t \to T) \to 0$, i.e., the system biomass of the system saturates before the end of the cycle.

We define $x_\alpha(j) \equiv \log(\rho_\alpha^{(j)}(t=0))$, and $q_\alpha(x,\eta) = \int_{\eta_0}^{\eta} \frac{r_\alpha}{\dot{\eta}} d\eta$. This gives us $x(j+1) = x(j) + q(x(j), \eta_{\max}) + \log\delta$. First, we prove that $\frac{\partial q_A(x,\eta)}{\partial x_A} < 0$.

$$\frac{\partial q_A(x,\eta')}{\partial x_B} = \frac{\partial}{\partial x_B}\int_{\eta_0}^{\eta'} \frac{r_A(\eta)}{\dot{\eta}} d\eta \tag{S85}$$

$$= \int_{\eta_0}^{\eta'} \sum_C \frac{\partial}{\partial \rho_C}\left(\frac{r_A(\eta)}{\dot{\eta}}\right) \frac{\partial \rho_C}{\partial x_B} d\eta. \tag{S86}$$

For $\frac{\partial q_A(x)}{\partial x_A} < 0$, it is sufficient if $\frac{\partial \dot{\eta}}{\partial \rho_\alpha} > 0 \ \forall \alpha$. As an example, we take $\eta \equiv \sum_\alpha \rho_\alpha$.

$$\implies \frac{\partial q_A(x,\eta')}{\partial x_B} = \int_{\eta_0}^{\eta'} \sum_C \frac{\partial}{\partial \rho_C}\left(\frac{r_A}{\sum r_\alpha \rho_\alpha}\right)\frac{\partial \rho_C}{\partial x_B} d\eta \tag{S87}$$

$$= \int_{\eta_0}^{\eta'} \sum_C \frac{\partial^2 \log \sum_\alpha r_\alpha \rho_\alpha}{\partial \rho_C \partial \rho_A}\frac{\partial \rho_C}{\partial x_B} d\eta. \tag{S88}$$

We note that by Jensen's inequality, if $r_\alpha > 0$ is independent of ρ_α, $\ln \sum_\alpha r_\alpha \rho_\alpha$ is concave, i.e., $\partial_C \partial_A \ln \sum_\alpha r_\alpha \rho_\alpha < 0$. Later, we will explore the case that r_α is not independent of ρ_α.

$$\rho_C(\eta) = \exp\left(x_C + q_C(x,\eta)\right) \implies \frac{\partial \rho_C}{\partial x_B} = \left(\delta_{BC} + \frac{\partial q_C(x,\eta)}{\partial x_B}\right)\rho_C(\eta) \tag{S89}$$

$$\implies \frac{\partial q_A(x,\eta')}{\partial x_B} = \int_{\eta_0}^{\eta'} \sum_C \frac{\partial^2 \log \sum_\alpha r_\alpha \rho_\alpha}{\partial \rho_C \partial \rho_A}\left(\delta_{BC} + \frac{\partial q_C(x,\eta)}{\partial x_B}\right)\rho_C d\eta \tag{S90}$$

$$\implies \frac{d}{d\eta}\frac{\partial q_A(x,\eta)}{\partial x_B} = \frac{1}{\rho_A}\sum_C \frac{\partial^2 \log \sum_\alpha r_\alpha \rho_\alpha}{\partial \rho_C \partial \rho_A}\rho_A \rho_C \left(\delta_{BC} + \frac{\partial q_C(x,\eta)}{\partial x_B}\right). \tag{S91}$$

If we construct a matrix Q such that $Q_{A,B}(\eta) = \frac{\partial q_A(x,\eta)}{\partial x_B}$, a matrix H such that $H_{A,C} = \frac{\partial^2 \log \sum_\alpha r_\alpha \rho_\alpha}{\partial \rho_C \partial \rho_A}\rho_A \rho_C$, and a matrix D such that $D_{A,B} = \delta_{A,B}/\rho_A$ the equation turns to

$$\frac{dQ}{d\eta} = DH(I+Q). \tag{S92}$$

First, we note that DH is similar to $D^{1/2}HD^{1/2}$, which is symmetric and negative definite by Sylvester's law. Thus, DH is also negative definite as similar matrices share eigenvalues. Further, HD is also negative definite with the same eigenvalues. Consider the candidate Lyapunov function $((I+Q)_A)^2$ where Q_A is one of the rows of Q.

$$\frac{d|(I+Q)_A|^2}{dt} = \frac{dQ_\alpha}{dt}(I+Q)_A + (I+Q)_A\frac{dQ_\alpha}{dt} \tag{S93}$$

$$= (I+Q)_A^T HD(I+Q)_A + (I+Q)_A^T DH(I+Q)_A \tag{S94}$$

$$= (I+Q)_A^T(HD+DH)(I+Q)_A < 0. \tag{S95}$$

This implies that $(I+Q)_A$ is Lyapunov stable and thus $|(I+Q)_A| < 1$ as $Q(0) = 0$. This implies that $0 > Q_{\alpha,\alpha} > -2 \ \forall \alpha$

E.4. Stability of the Fixed Point. Now consider the candidate discrete-time Lyapunov function, $V = (x - x^*)^2$, where x^* is the steady-state solution (for now we consider the species that survive, i.e., there exists an x^* such that $q_\alpha(x^*, \eta_{\max}) = -\log\delta \ \forall \alpha$).

$$V(x(j+1)) - V(x(j)) = (x(j+1) - x^*)^2 - (x(j) - x^*)^2 \tag{S96}$$

$$= x(j+1)^2 - x(j)^2 - 2x^* \cdot (x(j+1) - x(j)) \tag{S97}$$

$$= (q(x(j),T) + \log\delta)^2 + 2x(j)\cdot(q(x(j),\eta_{\max}) + \log\delta) \tag{S98}$$

$$- 2x^* \cdot (q(x(j),\eta_{\max}) + \log\delta) \tag{S99}$$

$$= (q + \log\delta)\cdot(q + \log\delta + 2(x - x^*)) \tag{S100}$$

$$= \sum_\alpha (q_\alpha(x) + \log\delta)\cdot(q_\alpha(x) + \log\delta + 2(x_\alpha - x_\alpha^*)). \tag{S101}$$

Define $\bar{q}_\alpha(x) \equiv q_\alpha(x) + 2(x_\alpha - x_\alpha^*)$. Thus, $\bar{q}_\alpha(x^*) = 0$ and $\partial_\alpha \bar{q}_\alpha(x) > 0$. For all values of $x_{\beta\neq\alpha}$:

$$\bar{q}_\alpha(x) + \log\delta > 0 \quad \text{for } x_\alpha > x_\alpha^*, \quad \bar{q}_\alpha(x) + \log\delta < 0 \quad \text{for } x_\alpha < x_\alpha^*. \tag{S102}$$

$$q_\alpha(x) + \log\delta < 0 \quad \text{for } x_\alpha > x_\alpha^*, \quad q_\alpha(x) + \log\delta > 0 \quad \text{for } x_\alpha < x_\alpha^*. \tag{S103}$$

Thus, $(q_\alpha + \log\delta)\cdot(q_\alpha + 2(x_\alpha - x_\alpha^*) + \log\delta) < 0$. and the candidate Lyapunov function, $V(x)$, always decreases and the system converges to x^*.

E.5. Existence and Uniqueness of the Fixed Point. The fixed point must also be unique, as this is a non-linear complementarity problem (NCP) for the mapping $f(\vec{\rho}) = q + \log\delta$, and it is well-known that there exists a unique solution to a NCP if the mapping is monotone (28). This result can be intuitively understood by assuming, for contradiction, that there exist two distinct equilibria x^* and y^* such that

$$q(x^*) = 0 \quad \text{and} \quad q(y^*) = 0.$$

Since $x^* \neq y^*$, there exists at least one coordinate α such that $x^*_\alpha \neq y^*_\alpha$. Without loss of generality, assume $x^*_\alpha > y^*_\alpha$. Since q_α is strictly decreasing in all coordinates, adjusting other x_β to maintain $q_\alpha(x) = 0$ affects the other equilibrium conditions $q_\beta(x) = 0$ for $\beta \neq \alpha$. This interdependence makes it impossible to have two distinct equilibria without violating at least one $q_\beta(x) = 0$ condition.

Thus, the system is globally stable, converging to the same fixed point independent of the initial condition. We note that this proof can be extended to the case when some species do not survive, by taking $z_\alpha = \max\{-K, x_\alpha\}$ where $\exp(-K)$ is the lower population bound for the species to be considered present. This is still an NCP with a unique solution.

E.6. Initial-condition dependent growth rates. This analysis will also allow us to explore the cases where r_α can change with ρ_α in a multi-dimensional space. Since the proof above rests on the fact that $\ln\vec{r}\cdot\vec{\rho}$ is concave, we consider when this concavity no longer holds. Consider $\vec{r}$ where each element is r_α, and $\vec{\rho}$, where each element is ρ_α.

$$\Delta \ln\vec{r}\cdot\vec{\rho} = \frac{2\left(\nabla\cdot\vec{r}\right) + \vec{\rho}\cdot\left(\Delta\vec{r}\right)}{\vec{r}\cdot\vec{\rho}} \;-\; \frac{|\vec{r} + (\nabla\vec{r})^T\cdot\vec{\rho}|^2}{(\vec{r}\cdot\vec{\rho})^2} \qquad \text{[S104]}$$

To find when $\Delta\ln\vec{r}\cdot\vec{\rho} < 0$, we analyze a perturbation around a constant $\vec{r}$. Assume that $\vec{r}(\vec{\rho})$ is close to a constant vector $\vec{r}_0$, such that $\vec{r}(\vec{\rho}) = \vec{r}_0 + \delta\vec{r}(\vec{\rho})$, where $|\delta\vec{r}(\vec{\rho})| \ll |\vec{r}_0|$. Substituting $\vec{r} = \vec{r}_0 + \delta\vec{r}$ into the general Laplacian expression:

$$\begin{aligned}\Delta \ln\vec{r}\cdot\vec{\rho} &= \frac{2\left(\nabla\cdot(\vec{r}_0+\delta\vec{r})\right) + \vec{\rho}\cdot\left(\Delta(\vec{r}_0+\delta\vec{r})\right)}{(\vec{r}_0+\delta\vec{r})\cdot\vec{\rho}} - \frac{|\vec{r}_0+\delta\vec{r}+(\nabla(\vec{r}_0+\delta\vec{r}))^T\cdot\vec{\rho}|^2}{((\vec{r}_0+\delta\vec{r})\cdot\vec{\rho})^2}.\\ &= \frac{2\left(\nabla\cdot\delta\vec{r}\right) + \vec{\rho}\cdot\left(\Delta\delta\vec{r}\right)}{\vec{r}_0\cdot\vec{\rho}+\delta\vec{r}\cdot\vec{\rho}} - \frac{|\vec{r}_0+\delta\vec{r}+(\nabla\delta\vec{r})^T\cdot\vec{\rho}|^2}{(\vec{r}_0\cdot\vec{\rho}+\delta\vec{r}\cdot\vec{\rho})^2}.\end{aligned}$$

To first order in $\delta\vec{r}$:

$$\begin{aligned}\Delta\ln\vec{r}\cdot\vec{\rho} &\approx \frac{2\left(\nabla\cdot\delta\vec{r}\right)+\vec{\rho}\cdot\left(\Delta\delta\vec{r}\right)}{\vec{r}_0\cdot\vec{\rho}} - \frac{|\vec{r}_0|^2 + 2\,\vec{r}_0\cdot(\delta\vec{r}+(\nabla\delta\vec{r})^T\cdot\vec{\rho})}{(\vec{r}_0\cdot\vec{\rho})^2 + 2(\vec{r}_0\cdot\vec{\rho})(\delta\vec{r}\cdot\vec{\rho})}\\ \Delta\ln\vec{r}\cdot\vec{\rho} < 0 &\iff 2\left(\nabla\cdot\delta\vec{r}\right)+\vec{\rho}\cdot\left(\Delta\delta\vec{r}\right) < \frac{|\vec{r}_0|^2 + 2\,\vec{r}_0\cdot(\delta\vec{r}+(\nabla\delta\vec{r})^T\cdot\vec{\rho}) - 2|\vec{r}_0|^2(\delta\vec{r}\cdot\vec{\rho})/(\vec{r}_0\cdot\vec{\rho})}{\vec{r}_0\cdot\vec{\rho}}\\ &\impliedby 2\left(\nabla\cdot\delta\vec{r}\right)+\vec{\rho}\cdot\left(\Delta\delta\vec{r}\right) < \frac{|\vec{r}_0|^2 + 2\,\vec{r}_0\cdot(\delta\vec{r}+(\nabla\delta\vec{r})^T\cdot\vec{\rho}) - 2|\vec{r}_0|^2(\delta\vec{r}\cdot\vec{\rho})/(\vec{r}_0\cdot\vec{\rho})}{|\vec{r}_0||\vec{\rho}|}\\ &\impliedby 2\left(\nabla\cdot\delta\vec{r}\right)+\vec{\rho}\cdot\left(\Delta\delta\vec{r}\right) < \frac{|\vec{r}_0| - 2|(\delta\vec{r}+(\nabla\delta\vec{r})^T\cdot\vec{\rho})| - 2|\vec{r}_0||\delta\vec{r}|}{|\vec{\rho}|}\\ &\impliedby |\nabla\cdot\delta\vec{r}| + \frac{|\vec{\rho}||\Delta\delta\vec{r}|}{2} + \frac{|\delta\vec{r}|}{|\vec{\rho}|} + ||(\nabla\delta\vec{r})^T||^* + \frac{|\vec{r}_0||\delta\vec{r}|}{|\vec{\rho}|} < \frac{|\vec{r}_0|}{2|\vec{\rho}|}\end{aligned}$$

where $||A||^* = \sup_{|\vec{\rho}|=1}||Ax||$ is the operator norm. Define $\epsilon \equiv \frac{|\delta\vec{r}|}{|\vec{r}_0|}$ and a characteristic frequency scale f over which $\delta\vec{r}$ varies, and noting that $|\vec{\rho}| \lesssim 1$, the conditions become:

$$2\frac{\epsilon}{f} + \frac{\epsilon}{2f^2} + 2\epsilon < \frac{1}{2} \iff \sqrt{\epsilon} < \frac{f}{2f+1} < f.$$

Thus, we require that $f > \sqrt{\epsilon}$, or $|\vec{r}_0| > \Delta\delta\vec{r}$.

E.7. Existence of non-trivial solutions can be inferred by mutual invasibility. Inferring when a possible frequency exists such that $q = 0$ can be very complicated because the time dependence of the growth rates cannot be inferred without solving the ODEs numerically. However, because we know there is a negative frequency dependence, we can infer if such an x^* exists by asking what the values of $q(0)$ and $q(1)$ are. If $q > 0$ for all x, that would mean that Species A always has a fitness advantage over Species B. Similarly, if $q < 0$ for all x, that would mean that Species B always has a fitness advantage over Species A.

The ability to understand the necessary and sufficient conditions for coexistence by considering only the cases that either species is present (as $x = 0$ is the case when only Species B is present, and $x = 0$ is the case when only Species A is present) is very valuable when studying systems with non-linear growth rates. The study of these cases, also known as invasion analysis, is ordinarily sufficient to demonstrate coexistence. But because of the result that $q' < 0$, it is also necessary.

For our case, mutual invasibility can be verified without any numerical simulations. This is because the condition $q = 0$ can be written as $\mathbb{E}(r_A/r_B) > 1$, where $\mathbb{E}(\cdot)$ is the time-averaged expectation value. Mathematically, $\mathbb{E}(\cdot)$ is the integral of the argument from the lowest biomass value to the highest biomass value attained in the monoculture, weighted by

$\omega(s) \equiv [-\log\delta \cdot (\frac{n_0}{1-\delta} - s)]^{-1}$. $\omega(s)$ is the equivalent of the partition function for biomass accumulation. Similarly, $q(1) < 0$ can we written as $\mathbb{E}(r_B/\bar{r}) > 1$. If all monocultures are invadable, then there necessarily is coexistence.*

This criterion provides a general intuition of when there is coexistence: when both r_A/r_B and r_B/r_A are large for different parts of the growth step, both monocultures are invadable and there is coexistence. Thus, we need a range of biomass values when A grows much faster than B, and a range when B grows much faster than A. Various trade-offs can facilitate such a separation of biomass ranges, as does the strength of the non-linearity. This indicates to us why coexistence is increased when biologically-motivated modifications are introduced.

This criterion also indicates when interactions between two species can facilitate coexistence: when the interactions between two species lead to the initially slower-growing species eventually growing faster than the initially faster-growing species. This is highlighted in Amarnath et al. (29) showing how stress-induced cross-feeding leads to stable coexistence in a marine co-culture. Species A grows faster than Species B initially, but then pollutes its environment by secreting acetate as a by-product of growth. This pollution leads to the supression of its own growth and the leakage of metabolites. Species B can thus consume these metabolites to grow. Thus, this leads to the creation of periods when A grows much faster than B, and a period when B grows much faster than A. Though the experiment was performed in growth-dilution cycles, in natural settings the periodic supply of food describes a very similar dynamic in the system. The experimental result was surprising because if the coexistence were due to the standard picture of commensal/mutualistic cross-feeding where one species steadily secretes a metabolite consumed by the other, there would be no coexistence for this pair of species as under ideal conditions, one species always grows faster than the other.

Thus, this mutual invasibility criterion provides a counter-point to the standard conception of coexistence due to mutualism in which both species promote each others' growth. In time varying environments, both species can end up limiting their own growth rates and thus coexist. This suggests that self-organized mechanisms by which species inhibit their own growth may facilitate coexistence.

E.8. Stabilization of Resource Trajectories. But we emphasize that from a phenomenological point of view, this assumption can be viewed as the minimal closure of the equations describing an ecosystem that results in closed form self-consistency criterion. In Supplementary Text S2E, we show that if the growth rates are not too susceptible to changes in frequency (exactly, $\Delta\delta r_\alpha \ll r_\alpha^0$ where $r_\alpha = r_\alpha^0 + \delta r_\alpha$ and the gradient is with respect to changes in frequencies), then the local stability criterion of Eq. **S84** indeed becomes a global criterion and thus provides a necessary and sufficient criterion for a species to persist in the community. Crucially, this criterion is independent of the functional dependence of $r_\alpha(\eta)$ on η. This allows us to rewrite Eq. **S84** as

$$I_\alpha \equiv \int_{\eta^{\not\alpha}(0)}^{\eta^{\not\alpha}(T)} \frac{r_\alpha(\eta^{\not\alpha}(t))}{d\eta^{\not\alpha}/dt} d\eta > -\log(\delta). \qquad [S105]$$

where $\eta^{\not\alpha}$ is the eco-coordinate of the community in the absence of α. We require the inequality in *Eq.* **S105** to hold for any one such cultures (see *Supplementary Text S2.6*). This significantly simplifies Eq. **S84** as we no longer need to find the exact steady state cycle η^{ss} A different perspective on the stabilizing nature of resource sharing can be obtained by looking at the trajectory that the co-culture traverses in the space of environmental variables. The key feature in the consumer-resource models that we use is that the trajectory is determined by the growth of the species. This is because the populations affect the environment through growth (either by consuming resources or secreting pollutants). Let us consider perturbations to the resource trajectory corresponding to a fixed point. Higher growth during a section of the trajectory means faster movement along the trajectory and less time spent at that section. But growth is also proportional to the time spent along the resource trajectory. Conversely, slower growth means more time at that section and thus the initial perturbation is countered. This leads to negative feedback for growth and, as a result, for resource change, thus stabilizing the resource trajectory. For the case of many environmental variables, movement along the trajectory can be projected onto the axis corresponding to each environmental variable, and the trajectory along each environmental variable can be considered independently. As movement along each projection is stabilized independently (such that at every point in time, there is a unique stable value of each environmental coordinate), the entire trajectory is stabilized.

A similar understanding can be obtained by considering perturbations in the resource trajectory itself rather than perturbations in growth as we did above. A perturbation in the resource trajectory will either slow down or speed up growth, and this perturbation in growth will counteract the original perturbation in the resource trajectory.

However, this stabilization is local along every point on the resource trajectory, while coexistence is a global property of the entire trajectory. In other words, a negative frequency dependence of fitness does not mean that fitness ever has to be negative. Coexistence requires that each species have a negative fitness over the other species for some frequency, especially when it is abundant. This leads us to a simple necessary and sufficient criterion for coexistence: mutual invasibility (discussed in Section F.

*This also allows us to see that there cannot be bistability, as that would require that $\mathbb{E}(r_A/r_B) < 1$ and $\mathbb{E}(r_B/r_A) < 1$ but $\mathbb{E}(r_A/r_B) + \mathbb{E}(r_B/r_A) > 2$ for all r_B and r_A as $x + 1/x > 2$ for all $x > 0$.

F. Mutual invasibility criterion. Here, we derive the criterion presented in Eq. **3**. Let's consider a monoculture of Species A with a minimal amount of Species B such that $(\rho_A^{(j)}(0), \rho_B(0)) = (\rho_A^0, \epsilon)$ and $\rho_A^0 \gg \epsilon$. Thus,

$$\log \frac{\rho_B^{(j+1)}(0)}{\rho_B^{(j)}(0)} = \int_0^T r_B(\rho_{\text{tot}}(t)) \cdot dt + \log \delta \tag{S106}$$

Since ρ_{tot} is monotonic in t, we can substitute t with ρ_{tot}

$$= \int_0^T \frac{r_B(\rho_{\text{tot}}) \cdot d\rho_{\text{tot}}}{d\rho_{\text{tot}}/dt} + \log \delta \tag{S107}$$

$$= \int_{\rho_A^0+\epsilon}^{\rho_{\text{tot}}^{\max}} \frac{r_B(\rho_{\text{tot}})}{r_A(\rho_{\text{tot}}) \cdot \rho_A^{(j)}(t)(\rho_{\text{tot}}) + r_B(\rho_{\text{tot}}) \cdot \rho_B^{(j)}(t)(\rho_{\text{tot}})} d\rho_{\text{tot}} + \log \delta \tag{S108}$$

Assuming $r_A(\rho_{\text{tot}}) > 0$, we can always choose ϵ such that $\rho_B^{(j)}(\rho_{\text{tot}}) \ll \rho_A^{(j)}(\rho_{\text{tot}})$, $\forall \rho_{\text{tot}}$, and thus $\rho_B^{(j)}(\rho_{\text{tot}}) \ll \rho_A^{(j)}(\rho_{\text{tot}}) \cdot r_A(\rho_{\text{tot}})/r_B(\rho_{\text{tot}})$ and $\rho_{\text{tot}} = \rho_A^{(j)}(\rho_{\text{tot}})$

$$\approx \int_{\rho_A^0}^{\rho_{\text{tot}}^{\max}} \frac{r_B(\rho_{\text{tot}})}{r_A(\rho_{\text{tot}})} \frac{d\rho_{\text{tot}}}{\rho_{\text{tot}}} + \log \delta. \tag{S109}$$

Similarly,

$$\log \frac{\rho_A^{(j+1)}(0)}{\rho_A^{(j)}(0)} \approx \int_{\rho_A^0}^{\rho_{\text{tot}}^{\max}} \frac{r_A(\rho_{\text{tot}})}{r_A(\rho_{\text{tot}})} \frac{d\rho_{\text{tot}}}{\rho_{\text{tot}}} + \log \delta = \log \rho_{\text{tot}}^{\max} - \log \rho_A^0 + \log \delta \tag{S110}$$

$$\implies \rho_A^{(j+1)}(0) = \delta \rho_{\text{tot}}^{\max}. \tag{S111}$$

Thus, in subsequent cycles,

$$\log \frac{\rho_B^{(j+k+1)}(0)}{\rho_B^{(j+k)}(0)} \approx \int_{\delta\rho_{\text{tot}}^{\max}}^{\rho_{\text{tot}}^{\max}} \frac{r_B(\rho_{\text{tot}})}{r_A(\rho_{\text{tot}})} \frac{d\rho_{\text{tot}}}{\rho_{\text{tot}}} + \log \delta. \tag{S112}$$

$$\implies \log \frac{\rho_B^{(j+k+1)}(0)}{\rho_B^{(j)}(0)} \approx k \int_{\delta\rho_{\text{tot}}^{\max}}^{\rho_{\text{tot}}^{\max}} \frac{r_B(\rho_{\text{tot}})}{r_A(\rho_{\text{tot}})} \frac{d\rho_{\text{tot}}}{\rho_{\text{tot}}} + \int_{\rho_A^0}^{\rho_{\text{tot}}^{\max}} \frac{r_B(\rho_{\text{tot}})}{r_A(\rho_{\text{tot}})} \frac{d\rho_{\text{tot}}}{\rho_{\text{tot}}} + (k+1) \log \delta \tag{S113}$$

For $k \to \infty$,

$$\rho_B^{(j+k+1)}(0) \gg \epsilon \text{ if } I_{A,B} \equiv \int_{\delta\rho_{\text{tot}}^{\max}}^{\rho_{\text{tot}}^{\max}} \frac{r_B(\rho_{\text{tot}})}{r_A(\rho_{\text{tot}})} \frac{d\rho_{\text{tot}}}{\rho_{\text{tot}}} > \log \delta. \tag{S114}$$

This is the invasibility criterion in Eq. **3**. If both $I_{A,B} > \log \delta$ and $I_{B,A} > \log \delta$, then there must be a non-trivial fixed point of the system, and by the proof in Section E, it must be stable and further, the only stable solution.

G. Continuous Growth Relations.

G.1. Monod Relation. A popular choice in microbiology and ecology for r_i is the Monod relation (30), also known as the Michaelis-Menten function or the Holling's type II functional response. It is chosen to describe growth that is proportional to the nutrient availability at low nutrient concentrations but saturates at high nutrient concentrations to a maximal rate.

We first consider the effect of varying the two environmental parameters, s_0 and δ for Species A and B with growth rates as described in Fig. S6A. We simulated six-hours long growth dilution cycles. In general, we find that the system is in the vicinity of a steady-state in less than ~ 100 cycles (our results did not change significantly for longer cycles or for more cycles). The steady-state cycle is defined as having population densities and nutrient concentrations that are exactly the same in consecutive cycles.

As can be seen in Fig. S6A for our choice of physiological parameters ($r_i^{\max}$ and K_i), Species A (shown in red) has a higher growth rate than Species B (shown in blue) when the nutrient concentration is high (because $r_A^{\max} > r_B^{\max}$), while Species B has a higher growth rate when the nutrient concentration is low (because $K_A^{\max} > K_B^{\max}$). Such a trade-off is known as the opportunist-gleaner trade-off (31). Although the empirical existence of such a trade-off is debated (32–34), we note that in this simplest case which has no other interactions, such a trade-off is necessary for coexistence as otherwise one species will always have a lower growth rate than the other and thus eventually be out-competed.

In Fig. S6B, we report the average fitness (average difference in growth rate over one cycle) of Species A over Species B after 100 cycles for different environmental parameters. A positive fitness value (denoted by red shading) indicates that the population of Species A is driving the population of Species B down, and thus Species B will eventually be removed from the system. A negative fitness value (denoted by blue shading) indicates that the population of Species A is being driven down and will eventually be removed from the system, while a near-zero fitness value (denoted by white shading) means that both species

have reached a non-zero steady state population and thus will coexist indefinitely. As can be seen and as would be expected, high nutrient supply favors the species with the higher value of $r_i^{\max}$, while low nutrient supply favors the species with the lower K_i. Similarly, a lower dilution factor favors the species with the higher value of $r_i^{\max}$ as the relative amount of time spent in higher nutrient concentrations is higher.

We also report the average fitness of Species A over Species B for different physiological parameters and fixed environmental parameters ($\delta = 0.1, s_0 = 10K_B$) in Fig. S6C. As would be expected, if there is no opportunist-gleaner trade-off, as in the top left and bottom right quadrants of the phase plot, there would be no coexistence. Further, even if there is a trade-off, coexistence is not guaranteed as can be seen in the other two quadrants which have red, white, and blue regions. Thus, coexistence is not a trivial consequence of the trade-off. However, there is a narrow parameter regime of coexistence between the region where Species A dominates and where Species B dominates.

In 1972, Stewart and Levin showed mathematically that two species with an opportunist-gleaner trade-off may coexist indefinitely in growth-dilution cycles (Fig. 1C).They also demonstrated that such a coexistence was "structurally stable", i.e., it was robust to noise in the environmental/experimental parameters (Fig. S6B). As can be seen, this coexistence is also robust to small physiological perturbations (Fig. S6C) and there exists an entire region in the environmental and physiological parameter phase space (shaded in white) where the two species coexist, rather than just being a boundary between the two regions. This is a key result as it shows that this kind of coexistence is not a result of narrow fine-tuning, but seems to incorporate stabilizing mechanisms that promote coexistence. While this was a crucial novel result, it has been mostly dismissed in literature (31), due to the relatively small region of coexistence in parameter phase space. However, as we will see below, this region of coexistence is significantly broadened when biologically-realistic effects are considered. As such, it indicates a more general emergent principle for self-stabilized coexistence rather than serving as just a niche special case.

G.2. Cut-off due to Maintenance Energy. Bacterial species require a certain minimum amount of energy, known as maintenance energy, to be able to grow. If sufficient non-zero amount of nutrients to generate this energy are not supplied, the bacteria cease to grow. This effect can be incorporated by subtracting a constant value of maintenance energy consumption rate, given by J_i, from the growth rate of each species and setting the minimal growth rate to be 0 (i.e, we exclude death). This leads to the following form for the growth rate:

$$r_i(s) = r_i^{\max} \cdot \frac{s}{s + K_i} - J_i. \qquad [S115]$$

This expands the coexistence region of phase space considerably. In fact, for almost any two species defined by the physiological parameters r_i, K_i, and J_i, the coexistence region of the environmental phase-space occupies an entire half-plane (see Fig. S6E). This is because at very low resource concentrations, one of the species necessarily grows, while the other doesn't. The species that grows at very low resource concentrations will subsequently always survive for all environmental parameters.

The coexistence region in physiological parameter space is also extended, with species benefiting from even relatively minor differences in resource affinities. This is because strict coexistence only requires sufficient fold change between cycles rather than any minimal abundance.

G.3. Hysteretic Growth Kinetics. We note that the Monod relation is obtained empirically for a perfectly-adapted bacterial population, i.e., the bacterial population is grown at a static nutrient concentration and its growth rate is measured for that nutrient concentration. In a growth-dilution cycle, the bacterial population may not have adapted to the nutrient concentration it experiences at any instant as the nutrient concentration is constantly changing. This can be viewed as a hysteresis in the growth-rate due to the slow adaptation of the internal state of the cells that constitute the population. Similar hysteretic effects are modeled by the Droop model which is popular in studying algae (35) and is also seen in macroscopic organisms as a predator's searching, attacking, or handling efficiency often empirically increases as prey density increases. This is because the feeding response of organisms often display some form of learning behavior, as a predator must have a minimal encounters with its prey before the predator is maximally efficient at feeding on that prey item.

Such a growth dependence is known as a Type III functional response and is described by the Hill function Eq. **S116**,

$$r_i(s) = r_i^{\max} \cdot \frac{s^k}{s^k + (K_i)^k}, \qquad [S116]$$

where $k > 1$ is a positive number that denotes the number of minimal encounters the consumer must have with its food to increase its efficiency (36).

We note that the Monod relation is a special case of the Hill function (when $k = 1$), and increasing k leads to an increase in the coexistence region of phase-space (see the case of $k = 2$ shown in Fig. S6D-F).

G.4. Lag Time. Another effect that can be incorporated is the presence of a lag-time, such that both species do not grow for a short period of time at the beginning of each cycle. By design, the presence of lag times benefits the species with the shorter lag-time. This does not significantly increase (or decrease) the coexistence region of the physiological and environmental phase spaces but rather shifts it in favor of one species. We note that though previous studies (37) found coexistence and bistability for species with constant growth rates and lag times in growth-dilution cycles, these studies require the dilution step to be a bottleneck step such that the total initial population is fixed (which requires changing the dilution amount every cycle). These studies also required very large differences in the yield (of the factor of ∼100-1000) between the two species. In the absence of these two effects, the coexistence disappears for constant growth rates (38) but persists for nonlinear growth rates.

A result that has been indicated numerically by previous studies for the case of Monod growth (39–41) and is implicit in the phase diagrams of Fig. S6 is that there is no initial condition dependence in this system. Thus, there are only three steady-state possibilities that are determined by environmental and physiological parameters alone and hold for all initial conditions: that Species A eventually takes over the system, that Species B eventually does so, or that both species coexist indefinitely in a defined steady-state cycle. In other words, there is no bistability or multistability. We also note from Fig. S6 that coexistence is determined by all six parameters that effectively describe the system and that each parameter can be varied to lead to any of the three possible outcomes. This implies that the system cannot be described as being a trivial outcome of a simple characteristic of the environment or physiology of the two species, but requires an interplay of the environment and the physiologies. Thus, though it is necessary that the growth rate dependences of the two species intersect, it is far from sufficient.

We note that if all r_i are linear in the concentration of the nutrient (also known as a Holling's type I functional response), coexistence is not possible and only one species can survive (16). This is because one species will always grow faster than the other species and thus out-compete the other species over many cycles. Thus, nonlinear growth dependences on nutrient concentrations are required for coexistence and reflect a trade-off in the growth process.

Thus, we note that even for two species competing for a single nutrient, the coexistence region of parameter phase space is not necessarily small, but possibly a result of multiple physiological trade-offs between growth rate, resource affinity, adaptation time scale, and survivability in low resource conditions. For other systems shown in Fig. 1, the trade-offs could be due to susceptibility to a pollutant, cross-feeding, or anomalous response to environmental stress. Accordingly, growth-dilution cycles result in a consumer-resource analog to winnerless competition models, where transient dynamics enable multiple species to persist (42).

H. Derivation of Equi-abundance Solution. We take each species, α, to have growth rate r_- basally and r_+ in its preferred growth rate. In the steady cycle, we look for the solution where there are N species, each with abundance $1/N$. First, since this is the steady cycle, we require

$$\sum_i r_{\alpha,i} \cdot \tau_i = \log(1/\delta), \tag{S117}$$

where τ_i is the time spent passing through each niche i. Plugging in the growth rates, we have

$$r_+\tau_\alpha + r_-(T - \tau_+) = \log(1/\delta), \tag{S118}$$

where τ_α is the time spent in the preferred niche. Since the rest of the equation carries no parameters unique to species α, τ_α must be the same for all species. Thus, we have that

$$\tau \equiv \tau_\alpha = \frac{\log(1/\delta)}{r_+ + r_-(N-1)}, \ \forall\alpha \tag{S119}$$

Now, we seek to find $\Delta\eta_n$ for each niche. Since this is the biomass consumed by all species in that niche, we have

$$\Delta\eta_n = \underbrace{\sum_{i<n} \frac{1}{N}\exp((n-2)r_-\tau + r_+\tau)(\exp(r_-\tau)-1)}_{\text{Species that have a preferred niche before the nth niche}} + \underbrace{\frac{1}{N}\exp((n-1)r_-\tau)(\exp(r_+\tau)-1)}_{\text{Species that prefers the nth niche}} \tag{S120}$$

$$+ \underbrace{\sum_{i>n} \frac{1}{N}\exp((n-1)r_-\tau)(\exp(r_-\tau)-1)}_{\text{Species that have a preferred niche after the nth niche}} \tag{S121}$$

After some simplification,

$$\Delta\eta_n = \frac{\exp((n-1)r_-\tau)(\exp(r_-\tau)-1)}{N}\left(\sum_{i<n}\exp((r_+ - r_-)\tau) + \frac{\exp(r_+\tau)-1}{\exp(r_-\tau)-1} + \sum_{i>n} 1\right) \tag{S122}$$

$$\implies \Delta\eta_n = \frac{\exp((n-1)r_-\tau)(\exp(r_-\tau)-1)}{N}\left((n-1)\exp((r_+ - r_-)\tau) + \frac{\exp(r_+\tau)-1}{\exp(r_-\tau)-1} + N - n\right) \tag{S123}$$

In the case that the correction term is independent of n, i.e.,

$$n(\exp((r_+ - r_-)\tau) - 1) \ll \frac{\exp(r_+\tau)-1}{\exp(r_-\tau)-1} + N - \exp((r_+ - r_-)\tau), \tag{S124}$$

we have that

$$\Delta\eta_n \propto \exp(nr_-\tau) \implies \Delta\eta_n \sim \delta^{\frac{n}{p+N-1}} \tag{S125}$$

and the niche widths must be exponentially spaced. We now explore the cases where this is true. This is obviously the case if $r_+ = r_-$ as then $\exp((r_+ - r_-)\tau) - 1 = 0$.

In the case that $N \gg p \equiv \frac{r_+}{r_-} > 1$, we have that

$$\exp(r\tau) = \exp(\frac{r/r_- \cdot \log(1/\delta)}{p+N-1}) \approx 1 + \frac{r/r_- \log(1/\delta)}{N} \tag{S126}$$

Thus, the LHS in correction term is given by

$$n\left(\frac{p-1-\log(1/\delta)}{N}\right) \ll N \tag{S127}$$

while the RHS is given by

$$\frac{\frac{p-\log(1/\delta)}{N}}{\frac{1-\log(1/\delta)}{N}} + N - \frac{p-1-\log(1/\delta)}{N} - 1 \approx N. \tag{S128}$$

Thus, Eq. **S124** is satisfied. Also, in the case that $p \gg N > 1$,

$$\exp((r_+ - r_-)\tau \to \exp(r_+\tau) = \exp\left(\frac{\log(1/\delta)}{1+\frac{N-1}{p}}\right) \approx \frac{1}{\delta}. \tag{S129}$$

and

$$\exp(r_- \cdot \tau \to \exp\left(\frac{\log(1/\delta)}{p+N-1}\right) \approx 1 + \frac{\log(1/\delta)}{p+N-1}. \tag{S130}$$

Thus,

$$\Delta\eta_n = \frac{\exp((n-1)r_-\tau)}{N}\frac{\log(1/\delta)}{p+N-1}\left(n(1/\delta-1) + \frac{\frac{1}{\delta}-1}{\frac{\log(1/\delta)}{p+N-1}} + N - \frac{1}{\delta}\right) \tag{S131}$$

$$= \frac{\exp((n-1)r_-\tau)}{N}\log(1/\delta)\left(\frac{n(1/\delta-1)}{p+N-1} + \frac{\frac{1}{\delta}-1}{\log(1/\delta)} + \frac{N-\frac{1}{\delta}}{p+N-1}\right) \tag{S132}$$

$$\approx \frac{\exp((n-1)r_-\tau)}{N}\left(\frac{1}{\delta}-1\right) \propto \delta^{\frac{n}{p+N-1}} \tag{S133}$$

I. The diagonal preference model. Based on the equiabundance solution, we consider a "diagonal model" in growth preference, in which each niche n has a dominant species $\hat{\alpha}(n)$ whose growth rate $r_{\hat{\alpha}(n),n}$ well exceeds the growth rate of other species in that niche, and each species is dominant only in one unique niche.

We anticipate the equi-abundance case to be highly stable. We validated this expectation by creating ensembles of $r_{\alpha,n}$ and $\Delta\eta_n$ values fluctuating within $\pm 30\%$. Notably, every species persists in $\sim 80\%$ of scenarios with near equi-abundance (Fig. S6B, S6C). We also found that higher growth preference p species in its main niche (with the accompanying change in the exponential niche distribution) increased survival rates of over 95%. In fact, even with just a 3-fold growth preference and $\pm 30\%$ noise, all species remained in 45-65% of cases. This nonlinear reliance on growth preference indicates diminishing returns.

Yet, as Fig. S6D illustrates, the proportion of preserved species for a set growth preference (p) declines as species and niche counts rise. The drop depends on N/p (Fig. S6E), emphasizing enhanced competition from the growing collective of slow-growing species.

Alternatively, the priority effect can be overcome by having the species preferred in earlier niches take on reduced growth preferences but equal niche widths. We find that exponentially-distributed growth rates for species in their preferred niches,

$$r_+(n) \propto (1/\delta)^{n/(N+p-1)}, \qquad [S134]$$

with r_- fixed, retains a similar diversity (Fig. S6G, S6H) as for exponentially distributed niche widths (Fig. S6B, S6C). See Fig. S6.

Collectively, these results underscore the tremendous (exponential) growth advantage of species specializing in early niches if p is not too large, and hence the much higher relative dominance required for species specializing in the late niches to be maintained in the community.

J. Resource Sharing in Consumer-Resource Models in a Chemostat. One might interpret the states in the Community State (CS) Model as analogous to resources in a Consumer-Resource model. In the case of large communities, it leads to the question of how many species can be expected to coexist if N species shared N resources, with each species growing on multiple resources.

In the context of the CS Model, species coexist by occupying distinct niches, with niche width and overlap playing critical roles in determining community structure. Translating this to the CR model framework, we postulated that the allocation and consumption of resources could be a surrogate for these niche dynamics. Thus, we simulated the CR model in a chemostat. Each species was described by a consumption/growth matrix with diagonal elements set to 1 (such that each species invariably consumed a specific resource) and off-diagonal elements set randomly as 1 or 0 with the constraints described below. The growth rates, We considered two distinct cases:

$K_s = M$ Case: In this case, we fixed the number of species that show rapid growth per resource. This setup parallels a situation in the CS Model where each niche supports a similar number of species. The results can be seen in Supplementary Figure S7.

$K_n = M$ Case: In this case, we explored a scenario where each species is allocated a fixed number of resources, akin to each species in the CS Model occupying M niches. The results can be seen in Supplementary Figure S8.

K. Comparison to other models in microbial ecology. There are a wide range of models employed in microbial ecology, both verbal and mathematical. These models differ in many ways, such as the entities being modeled (nutrients, species, or metabolites), or the structure of relationships (linear equations, differential equations, or networks). In this section, we contrast existing ecological models, such as the gLV (generalized Lotka-Volterra) and CR (Consumer-REsource) models, and our approach (in the Community State Model (CSM) introduced below) on methodological features:

1. Nature of interactions: Models such as the gLV and CRM are *microscopic*, in that species dynamics are determined by interactions between the smallest entities in the model. For gLV it is between species, and for CRM is between species and resources. CSM is macroscopic, in that species dynamics are determined by interactions between the species and a global variable (for CSM, the community state, possibly indicated by the community biomass).

2. Direction of community assembly: gLV and CRM are *bottom-up*, i.e., they suppose knowledge of individual species and their interactions, and predicts the resulting features of the community assuming species do not change physiologically. The CSM is *top-down* as it supposes knowledge of species growth-rates in the community context, and predicts species abundances based on small perturbations of the community.

3. Relation to emprical data: Models such as CRM are *mechanistic* as they presume explicit knowledge of the underlying mechanisms, such as resource consumption/production rates, which makes them intractable in most experimental settings (43). gLV and CSM are *phenomenological*, in that they presume ignorance of underlying mechanisms and rely on inferring parameters from data. In gLV, the data is species abundances in different communities. This can be difficult experimentally and sensitive to model details, and high-dimensional fitting of noise data can be computationally challenging (44). On the other hand, parameters in the CSM (growth rates and transition points in biomass) are directly measured.

4. Time-dependence: The properties of species/resources in gLV and CRM stay constant over time, while in CSM, as physiological changes are the primary consideration, they significantly vary over time. Please note that the time-dependence of parameters does not imply that the system will be in or out of equilibrium. Even if parameters do not

change in time, the system could be out of equilibrium due to the lack of a stable fixed point, and even if the parameters change, the system could be in quasi-equilibrium if the parameters change faster than it takes for the system to equilibrate.

5. Dynamics: Often CRM and gLV models are solved at steady-state for mathematical simplicity and dynamics are ignored. The CSM does not admit a steady-state solution for non-trivial phases in a cycle and the dynamics must be preserved. While an inter-cycle steady-state can exist for CSM (which ignores what happens within a cycle), this steady-state cannot be solved for analytically as it requires solving a system of trancendental equation.

Further, the CSM cannot and does not seek to describe how coexistence emerges in community assembly from microscopic pairwise competitive and cooperative processes. Rather, the CSM presumes that the species coexist and tries to understand features of that coexistence such as its robustness and stability. As such, the CSM does not posit competition or cooperation as the drivers (or limiters) of coexistence, but rather that physiological change and complementarity of preferred environmental conditions are inevitable consequences of exponential growth. Taking a cue from the ecological principle of succession that has significantly influenced our construction of this model, fast-growing pioneer species of trees in a forest are able to grow rapidly following an ecological disturbance such as a wildfire. Such fast-growth limits the initial growth of secondary species by limiting light availability, but also promotes it by enriching the soil and eventually attracting herbivory and parasitic plants that primary species cannot tolerate but secondary species are more resilient to. This complex interaction between primary and secondary species of trees is difficult to be construed as either competitive or collaborative as it involves both. Instead, the emphasis is on inevitable physiological and environmental changes.

References

1. G Hardin, The competitive exclusion principle. *science* **131**, 1292–1297 (1960).
2. V Volterra, Variations and fluctuations of the number of individuals in animal species living together. *ICES J. Mar. Sci.* **3**, 3–51 (1928).
3. AJ Lotka, The growth of mixed populations: two species competing for a common food supply in *The golden age of theoretical ecology: 1923–1940*. (Springer), pp. 274–286 (1978).
4. GF Gause, *The Struggle for Existence: A Classic of Mathematical Biology and Ecology*. (Courier Dover Publications), (2019).
5. GF Gause, Experimental analysis of vito volterra's mathematical theory of the struggle for existence. *Science* **79**, 16–17 (1934).
6. GE Hutchinson, Population studies-animal ecology and demography-concluding remarks in *Cold Spring Harbor symposia on quantitative biology*. (COLD SPRING HARBOR LAB PRESS, PUBLICATIONS DEPT 1 BUNGTOWN RD, COLD SPRING ...), Vol. 22, pp. 415–427 (1957).
7. R MacArthur, R Levins, Competition, habitat selection, and character displacement in a patchy environment. *Proc. Natl. Acad. Sci. United States Am.* **51**, 1207 (1964).
8. RH MacArthur, EO Wilson, *The theory of island biogeography*. (Princeton university press), (2016).
9. R Levins, *Evolution in changing environments: some theoretical explorations*. (Princeton University Press) No. 2, (1968).
10. A Rescigno, IW Richardson, On the competitive exclusion principle. *The bulletin mathematical biophysics* **27**, 85–89 (1965).
11. J Grinnell, The origin and distribution of the chest-nut-backed chickadee. *The Auk* **21**, 364–382 (1904).
12. J Grinnell, The niche-relationships of the california thrasher. *The Auk* **34**, 427–433 (1917).
13. LB Slobodkin, Growth and regulation of animal populations, (Holt, Rinehart and Winston,), Technical report (1961).
14. SA Levin, Community equilibria and stability, and an extension of the competitive exclusion principle. *The Am. Nat.* **104**, 413–423 (1970).
15. RH MacArthur, Population ecology of some warblers of northeastern coniferous forests. *Ecology* **39**, 599–619 (1958).
16. RA Armstrong, R McGehee, Competitive exclusion. *The Am. Nat.* **115**, 151–170 (1980).
17. AL Koch, Competitive coexistence of two predators utilizing the same prey under constant environmental conditions. *J. Theor. Biol.* **44**, 387–395 (1974).
18. R McGehee, RA Armstrong, Some mathematical problems concerning the ecological principle of competitive exclusion. *J. Differ. Equations* **23**, 30–52 (1977).
19. R Levins, Coexistence in a variable environment. *The Am. Nat.* **114**, 765–783 (1979).
20. CS Holling, The components of predation as revealed by a study of small-mammal predation of the european pine sawfly1. *The Can. Entomol.* **91**, 293–320 (1959).
21. S Smale, On the differential equations of species in competition. *J. Math. Biol.* **3**, 5–7 (1976).
22. RA Armstrong, R McGehee, Coexistence of species competing for shared resources. *Theor. population biology* **9**, 317–328 (1976).
23. J Huisman, FJ Weissing, Biodiversity of plankton by species oscillations and chaos. *Nature* **402**, 407–410 (1999).
24. M Huston, A general hypothesis of species diversity. *The Am. Nat.* **113**, 81–101 (1979).
25. GG Mittelbach, BJ McGill, *Community ecology*. (Oxford University Press), (2019).
26. Z Wang, et al., Complementary resource preferences spontaneously emerge in diauxic microbial communities. *Nat. communications* **12**, 6661 (2021).

27. B Bloxham, H Lee, J Gore, Biodiversity is enhanced by sequential resource utilization and environmental fluctuations via emergent temporal niches. *PLOS Comput. Biol.* **20**, e1012049 (2024).
28. PT Harker, JS Pang, Finite-dimensional variational inequality and nonlinear complementarity problems: a survey of theory, algorithms and applications. *Math. programming* **48**, 161–220 (1990).
29. K Amarnath, et al., Stress-induced metabolic exchanges between complementary bacterial types underly a dynamic mechanism of inter-species stress resistance. *Nat. Commun.* **14**, 3165 (2023).
30. J Monod, The growth of bacterial cultures. *Annu. review microbiology* **3**, 371–394 (1949).
31. JP Grover, J HUDZIAK, JD Grover, *Resource competition*. (Springer Science & Business Media) Vol. 19, (1997).
32. T Kiørboe, MK Thomas, Heterotrophic eukaryotes show a slow-fast continuum, not a gleaner–exploiter trade-off. *Proc. Natl. Acad. Sci.* **117**, 24893–24899 (2020).
33. AD Letten, M Yamamichi, Gleaning, fast and slow: In defense of a canonical ecological trade-off. *Proc. Natl. Acad. Sci.* **118** (2021).
34. JW Fink, NA Held, M Manhart, Microbial population dynamics decouple growth response from environmental nutrient concentration. *Proc. Natl. Acad. Sci.* **120**, e2207295120 (2023).
35. H Wang, PV Garcia, S Ahmed, CM Heggerud, Mathematical comparison and empirical review of the monod and droop forms for resource-based population dynamics. *Ecol. Model.* **466**, 109887 (2022).
36. LA Real, The kinetics of functional response. *The Am. Nat.* **111**, 289–300 (1977).
37. M Manhart, BV Adkar, EI Shakhnovich, Trade-offs between microbial growth phases lead to frequency-dependent and non-transitive selection. *Proc. Royal Soc. B: Biol. Sci.* **285**, 20172459 (2018).
38. J Lin, M Manhart, A Amir, Evolution of microbial growth traits under serial dilution. *Genetics* **215**, 767–777 (2020).
39. FM Stewart, BR Levin, Partitioning of resources and the outcome of interspecific competition: a model and some general considerations. *The Am. Nat.* **107**, 171–198 (1973).
40. MT Wortel, Evolutionary coexistence in a fluctuating environment by specialization on resource level. *J. Evol. Biol.* **36**, 622–631 (2023).
41. HL Smith, Bacterial competition in serial transfer culture. *Math. biosciences* **229**, 149–159 (2011).
42. V Afraimovich, I Tristan, R Huerta, MI Rabinovich, Winnerless competition principle and prediction of the transient dynamics in a lotka–volterra model. *Chaos: An Interdiscip. J. Nonlinear Sci.* **18**, 043103 (2008).
43. K Zengler, BO Palsson, A road map for the development of community systems (CoSy) biology. *Nat. Rev. Microbiol.* **10**, 366–372 (2012).
44. JD Davis, DV Olivença, SP Brown, EO Voit, Methods of quantifying interactions among populations using lotka-volterra models. *Front. Syst. Biol.* **2**, 1021897 (2022).